

Pfadintegrale und Cluster

dem Fachbereich Physik
der Carl von Ossietzky Universität Oldenburg
zur Erlangung des Grades eines

Doktors der Naturwissenschaften (Dr. rer. nat.)

vorgelegte Dissertation von

Peter Borrmann

geboren am 5. Mai 1965
in Gelsenkirchen.

Erstreferent : Prof. Dr. Dr. Eberhard R. Hilf
Korreferent : Prof. Dr. David Tomanek
Korreferent : Prof. Dr. Alexander Rauh
Tag der Disputation : 17. Februar 1995

Inhalt

Teil 1	3
1 Einleitung	3
1.1 Cluster	5
1.2 Dirac, Feynman und Metropolis	9
1.2.1 Das Thermodynamische Pfadintegral	11
Bibliographie	14
Teil 2	18
2 Recursion formulas for quantum statistical partition functions	19
3 Path Integral Density Functional Theory	24
4 New enhancements to Feynmans Path Integral for fermions	33
5 Specific heat in the thermodynamics of clusters	40
6 How should thermodymanics for small sytems be done?	53
7 Magnetism of small transition metal clusters and the effects of isomerisation	67
8 Structure and Stability of polarized Li^3He_N^+ cluster ions	76
9 The structure of Small Clusters: Multiple Normal-Modes Modell	86
Danksagung	108
Curriculum vitae	109

Teil 1

Kapitel 1

Einleitung

Die Ergebnisse der Philosophie sind die Entdeckung irgendeines schlichten Unsinnns und Beulen, die sich der Verstand beim Anrennen an die Grenzen der Sprache geholt hat. Sie, die Beulen, lassen uns den Wert jener Entdeckung erkennen.

Ludwig Wittgenstein, Philosophische Untersuchungen.

Hielte es der Autor mit dem frühen Wittgenstein, der in seinem *Tractatus logico-philosophicus* letzten Satz "Worüber man nicht sprechen kann, darüber muß man schweigen" zu dem Schluß kommt, daß es unmöglich sei, einen einzelnen Sachverhalt oder gar die Welt exakt zu beschreiben, weil das hierzu zur Verfügung stehende Werkzeug, die Sprache, für diesen Zweck nicht geeignet ist, würde der Leser diese Zeilen nicht lesen. Indes folgen auf etwa einhundert Seiten die Beulen, die wir uns beim Anrennen unseres Geistes gegen verschiedene physikalische Fragestellungen zugezogen haben. Auch soll Obiges nicht als Entschuldigung für etwaige sprachliche Unzulänglichkeiten herangezogen werden.

Die für eine Dissertation etwas ungewöhnliche Form dieser Arbeit erfordert schon an dieser Stelle einige Worte der Erläuterung. Im ersten Teil dieser Arbeit, der aus dieser Einleitung besteht, soll der Leser mit dem Thema *Pfadintegrale und Cluster* vertraut gemacht werden. Der zweite Teil enthält eine Zusammenstellung verschiedener zu diesem Thema vom Autor – allein oder in Zusammenarbeit mit verschiedenen Kollegen – verfaßter Arbeiten.

In Unterkapitel 1.1 werden wir versuchen, mit Hilfe einiger typischer Fragestellungen der Clusterphysik die Faszination, die dieses Gebiet auf uns ausübt, dem Leser zu vermitteln. Unterkapitel 1.2 enthält eine kurze Einführung in die Pfadintegraltheorie und dient insbesondere dazu, den Leser mit der im zweiten Teil oft unkommentiert verwendeten Nomenklatur vertraut zu machen. Am Ende des ersten Kapitels findet sich eine umfangreiche nach Themenge-

bieten und Fragestellungen geordnete Literaturliste.

In Kapitel 2 wird eine Rekursionsformel für die effektive Berechnung von quantenstatistischen Zustandsummen vorgestellt, die gemeinsam mit G. Franke entwickelt wurde. Das dort dargestellte Ergebnis ist eine wesentliche Voraussetzung für die in Kapitel 3 dargestellte Pfadintegral-Dichtefunktional-Methode, in der erstmalig eine Verknüpfung der Pfadintegralmethode mit Dichtefunktionalen vorgeschlagen wird. Unter Ausnutzung der Rekursionsformel ergibt sich mit Hilfe dieser Verknüpfung eine neue Methodik, in der der numerische Rechenaufwand für Systeme, die der Bose-Einstein- oder Fermi-Dirac-Statistik unterliegen, nur mit dem Quadrat der Teilchenzahl N steigt.

In Kapitel 4 wird ein ähnliches, jedoch über einen sehr unterschiedlichen Zugang erzieltetes Ergebnis, dargestellt. Hier beruht die Reduzierung des numerischen Aufwandes nicht auf Anwendung einer Rekursionsformel. Eine sorgfältige Betrachtung der in speziellen Pfadintegral Monte-Carlo Algorithmen auftretenden Determinanten zeigt, daß diese mit einer Anzahl von N^2 und in speziellen Fällen sogar mit nur N statt N^3 Operationen berechnet werden können. Durch diese einfache algebraische Beobachtung konnten wir zeigen, daß auch in traditionellen Pfadintegral Monte-Carlo Algorithmen für Fermionen der numerische Rechenaufwand drastisch reduziert werden kann. Diese Ergebnisse wurden in Zusammenarbeit mit E.R. Hilf erzielt.

Die Kapitel 5 und 6 beschäftigen sich mit der Thermodynamik kleiner Systeme. In Kapitel 5, einem gemeinsam mit D. Gloski und E.R. Hilf erstellten Artikel, wird anhand eines Beispiels der Unterschied, der sich durch die Verwendung verschiedener thermodynamischer Ensembles für die höheren Momente der entsprechenden thermodynamischen Zustandfunktionen ergeben kann, diskutiert. Während bei makroskopischen Systemen solche Unterschiede in der Regel verschwinden, muß bei mesoskopischen Systemen die Frage, ob sich die Cluster bei einem Experiment in einem Wärmebad befinden – d.h. eine konstante Temperatur haben – oder aber die Energie der Cluster konstant ist, an den Experimentalphysiker gestellt werden. In dem in Kapitel 6 abgedruckten Artikel wird weiterhin die Frage diskutiert, auf welche Art und Weise mit verschiedenen Methodiken verbundene systematische Fehler umgangen werden können.

In Kapitel 7 werden die magnetischen Eigenschaften von kleinen Übergangsmetallclustern anhand eines einfachen thermodynamischen Modells studiert. Insbesondere wird die Kopplung der internen Struktur dieser Cluster mit einem externen magnetischen Feld und der Temperatur studiert. Diese gemeinsam mit E.R. Hilf, D. Tomanek und B. Diekmann verfaßte Arbeit ist eine Vorstudie zu einem Projekt, in dem die Frage, ob und wie *Clustermaterial* als

magnetischer Masseninformatiionsspeicher verwendet werden kann, behandelt wird.

In Kapitel 8 wird die Pfadintegral Monte-Carlo Methode auf polarisierte $\text{Li}^+ \text{}^3\text{He}_N$ Cluster angewendet. Durch Vergleich von die Fermi-Dirac Statistik berücksichtigenden und Boltzmann-statistischen Rechnungen wird hier gezeigt, wie sich die fermionische Natur von ${}^3\text{He}$ auf die Struktur und Energie der Cluster auswirkt. Weiterhin zeigen die Rechnungen, daß Cluster der Größe $N \geq 7$ sehr instabil sind und damit experimentell kaum beobachtbar sein sollten. Diese Arbeit wurde ebenfalls gemeinsam mit E.R. Hilf erstellt.

Kapitel 9 besteht aus einem Artikel, welcher einem Projekt unter Federführung von G. Franke und Mitarbeit von E.R. Hilf und dem Autor entsprungen ist. In ihm werden die thermodynamischen Eigenschaften von kleinen Argon Clustern mit Hilfe eines einfachen Oszillatormodells berechnet und mit den Ergebnissen aus Pfadintegralsimulationen verglichen. Es werden die Vorteile und Limitierungen dieses Modells diskutiert.

Im folgenden können und wollen wir weder einen kompletten Überblick über die Clusterphysik noch über die Theorie der Pfadintegrale geben. Vielmehr soll der Leser mit beiden Gebieten soweit vertraut gemacht werden, daß er in den Stand versetzt wird, die originären Beiträge des zweiten Teils dieser Arbeit in diese Gebiete einzuordnen, auch wenn dies nicht sein eigenes Arbeitsgebiet sein sollte.

1.1 Cluster

Als Cluster bezeichnet man allgemein *Ansammlungen oder Gruppen ähnlicher Dinge*. Wenn man über Cluster spricht, sollte man daher zunächst sagen, über welche Art von Clustern man redet.

In dieser Arbeit soll das Wort Cluster fortan räumliche Ansammlungen von einigen wenigen bis zu einigen hunderttausend Atomen oder Molekülen bezeichnen. Cluster bilden als mesoskopische Systeme somit quasi das Bindeglied zwischen den mikroskopischen Objekten, die in der Atom- und Molekülphysik betrachtet werden, und dem makroskopischen Festkörper.

Die teilweise vollkommen unterschiedlichen Eigenschaften von isolierten Atomen und Molekülen und aus diesen aufgebauten Festkörpern lassen eine Fülle von größenabhängigen Effekten für Cluster erwarten. Im folgenden wollen wir einige der typischen Fragestellungen der Clusterphysik kurz darstellen.

Wie entstehen Cluster ?

Die Frage des Clusterwachstums oder Aggregation ist eng mit der experimen-

tellen Herstellung von Clustern verknüpft. Freie Cluster werden zur Zeit durch drei sehr unterschiedliche Methoden produziert.

In Gasaggregationsquellen werden Atome oder Moleküle in ein Edelgas verdampft. Nach Abkühlung durch Kollisionsprozesse mit den Edelgasatomen lagern sich die Atome in diesen Quellen zu Clustern zusammen.

Bei der Gasstrahlexpansion wird ein heißes Gas unter hohem Druck ins Vakuum expandiert. Durch die adiabatische Expansion wird eine extreme Abkühlung bewirkt, und die Atome oder Moleküle kondensieren zu Clustern. Auf welcher Zeitskala und ob dieser Prozeß überhaupt stattfindet, ist stark von den thermodynamischen Variablen, z.B. dem Druck und der Temperatur des Edelgases abhängig.

Das dritte Verfahren basiert auf einem ähnlichen Prinzip. Hier werden die Cluster durch Beschuß einer Festkörperoberfläche mit Photonenstrahlen (Laserdesorption), sehr schnellen Ionen (Plasmadesorption) oder schnellen Ionen (Sputtering) von der Festkörperoberfläche desorbiert. Die hier stattfindenden Prozesse sind weder experimentell noch theoretisch abschließend geklärt, sondern Gegenstand aktueller Forschung. In erster Näherung können sie dadurch charakterisiert werden, daß sich im Bereich des Einschusses auf der Festkörperoberfläche eine hochangeregte Zone bildet, in der Atome oder ganze *Bruchstücke* des Festkörpers herausgeschleudert werden, die anschließend ähnlich wie in den obigen Methoden zu Clustern kondensieren bzw. durch Evaporation von Atomen und leichten Molekülen abkühlen.

Welche Struktur haben Cluster ?

Massenspektroskopische Untersuchungen an mit den o.g. Verfahren erzeugten Clustern haben gezeigt, daß verschiedene Clustergrößen mit besonderer Häufigkeit auftreten. Diese energetisch offensichtlich besonders günstigen Cluster werden als **magisch** bezeichnet. Die magischen Zahlen sind für verschiedene Clustersorten unterschiedlich und hängen von der Art der interatomaren Bindungen zwischen den Konstituenten des Clusters ab. Im einfachsten Fall (z.B. bei Edelgasclustern) lassen sich die magischen Zahlen als Schalenabschlüsse spezieller geometrischer Aufbauprinzipien konstruieren. Jedoch ist im allgemeinen Vorsicht geboten [32, 33]. Z.B. sind die energetischen Unterschiede bei kleinen Fe_N Clustern ($N < 100$) zwischen fcc und hcp Strukturen der gleichen Größe oft verschwindend gering. Schließlich haben wir gezeigt, daß sich in einem statistischen Ensemble mehrere Strukturen eines Clusters kohärent überlagern können.

Die Frage der stabilsten Struktur von Clustern kann z.Zt. meist nur mit theoretischen Methoden entschieden werden, da die herkömmlichen experimentellen Verfahren der Festkörperphysik zur Strukturbestimmung an Clusterstrahlen im Vakuum nicht durchführbar sind.

Welche elektromagnetischen Eigenschaften haben Cluster?

Die Frage nach den elektromagnetischen Eigenschaften von kleinen Teilchen

ist eng mit der Geburtsstunde der heutigen Clusterphysik verbunden. Im Jahre 1962 berechnete Kubo die Eigenschaften von in einem begrenzten Volumen eingeschlossenen Elektronen, die sich dort als stehende Wellen mit einem diskreten Energiespektrum verhalten. Der diskret, mittlere Niveauabstand des Energiespektrums liegt z.B. bei metallischen Teilchen von 100 Å Durchmesser bei $\delta = 1$ K. Wegen der hohen Coulombenergie in einem solch kleinen System muß das Teilchen bei niedrigen Temperaturen gleichzeitig neutral sein. Aus diesen beiden Eigenschaften lassen sich eine Fülle von weiteren Phänomenen ableiten.

In den letzten Jahren gilt den magnetischen Eigenschaften von Metallclustern besonderes Interesse. Die Anzahl der Veröffentlichungen zu diesem Gebiet ist kaum noch überschaubar. Hier findet man ein besonders gutes Beispiel für einen größenabhängigen Effekt. So sind Übergangsmetallcluster bis zu einer Größe von $N=30$ superparamagnetisch, d.h. sie haben ein, verglichen mit isolierten Atomen, sehr großes magnetisches Moment. Größere Cluster zeigen dann ferromagnetische oder antiferromagnetische Eigenschaften.

In Kapitel 6 wird ein einfaches thermodynamisches Modell vorgestellt, mit dessen Hilfe die Effekte berechnet werden können, die sich aus dem einfachen Fakt ergeben, daß kleine Übergangsmetallcluster in verschiedenen Strukturen mit vergleichbaren Grundzustandsenergien aber sehr verschiedenen mittleren magnetischen Momenten vorliegen können.

Welche spektroskopischen Eigenschaften haben Cluster?

Ein außergewöhnliches, oft zitiertes Beispiel für die ungewöhnlichen spektroskopischen Eigenschaften von Clustern ist bereits seit über 3500 Jahren bekannt. Ändert man die Größe von kolloidalen Silberclustern in einem Wasserglas von 0.1 bis 1.3 μm , so ändert sich die Farbe der Flüssigkeit von rot bis zu blau und grün (siehe [24] S. 549). Der Effekt wurde bereits 1908 von Mie [31] erklärt und beruht darauf, daß sich die Plasmaresonanzfrequenz der Metallelektronen in diesen Clustern abhängig von ihrer Größe ändert.

Die Laserspektroskopie an Clustern kann im Zusammenspiel mit theoretischen Rechnungen dazu genutzt werden, die Bindungsmechanismen in Clustern zu verstehen.

Wie ist Dynamik von Clustern?

Anders als bei Molekülen sind die Bindungen in Clustern oft relativ schwach, so daß bei vielen Clustertypen – insbesondere van der Waals Clustern – z.B. Strukturumwandlungen innerhalb eines dynamischen Prozesses möglich sind. Eine typische, die Dynamik von Clustern betreffende Frage ist z.B., warum Edelgascluster nach ihrer Erzeugung auf einer sehr kurzen Zeitskala in die Struktur, die dem absoluten Minimum der Born-Oppenheimer Oberfläche entspricht, relaxieren. Hierbei müssen die Cluster sozusagen durch eine sehr stark

zerfurchte Gestaltisomer-Potentialoberfläche mit sehr vielen Minima ihren Weg ins absolute Potentialminimum finden ¹.

Weitere Problemstellungen hängen stark mit der schon oben angesprochenen Herstellung von Clustern zusammen. Die Fusion von Clustern und die Spaltung eines Clusters sind z.B. dynamische Prozesse, die hierbei von Interesse sind.

Welche thermodynamischen Eigenschaften haben Cluster?

Zur vollständigen Beschreibung von Clustern müßten die oben genannten Eigenschaften jeweils für alle Größen und alle Temperaturen untersucht werden. Hier stellt sich zunächst die Frage, ob und wie die makroskopische Größe Temperatur für solch kleine Systeme wie Cluster überhaupt definiert ist. Auf diese Frage wird in den oben genannten Artikeln näher eingegangen. Aus experimenteller Sicht wird neuerdings die Frage, wie man ein Thermometer für kleine Systeme entwerfen kann, diskutiert.

Die theoretische Beschreibung von Clustern gestaltet sich sehr schwierig, weil die Anwendung mikroskopischer Methoden in der Regel äußerst aufwendig ist, da bei diesen Methoden der numerische Aufwand sehr schnell mit der Anzahl der Freiheitsgrade wächst ². Die Anwendung makroskopischer Methoden verbietet sich jedoch in vielen Fällen, da hierzu notwendige Voraussetzungen nicht erfüllt sind. Wesentlich hierbei ist, daß bei Clustern diskrete Effekte eine Rolle spielen, d.h. daß sich die Eigenschaften eines Clusters durch die Hinzufügung eines weiteren Partikels wesentlich ändern können, was offensichtlich einer der Grundannahmen in allen Modellen z.B. der Festkörperphysik widerspricht. Als Auswege aus diesem Dilemma bieten sich im wesentlichen zwei Strategien an.

Zum einen können *mean-field* Modelle aus der Kernphysik, die Oberflächeneffekte bzw. das Verhältnis von Oberfläche und Volumen berücksichtigen, entlehnt und weiterentwickelt werden. Zum anderen kann versucht werden, neue mikroskopische Verfahren zu entwickeln oder alte Verfahren so weiterzuentwickeln, daß mit diesen die zu untersuchenden Fragestellungen auf den heute zur Verfügung stehenden Rechenmaschinen bearbeitet werden können.

Im Moment muß die Clusterphysik sicherlich noch als Grundlagenphysik bezeichnet werden, da die derzeitige Forschung in den meisten Fällen noch weit von Anwendungen entfernt ist. Dennoch beginnt sich an einigen Stellen

¹Bei einem aus 13 Atomen bestehenden Argon Cluster liegt die Anzahl der lokalen Minima bereits bei ca. 1000, wenn man von einem Zweiteilchenpotential zwischen den Argon-Atomen ausgeht.

²Zum Beispiel ist der numerische Aufwand bei herkömmlichen Methoden der Quantenchemie in der Regel proportional zur vierten Potenz der Teilchenzahl.

die Lücke zu schließen.

In den letzten Jahren beginnt das Interesse an Clustermaterial, d.h. Festkörpern oder dünnen Schichten, die aus Clustern aufgebaut sind, stetig zu wachsen. Es besteht hier die Hoffnung, daß einige der speziellen Eigenschaften von Clustern auch in solchen Festkörpern in ähnlicher Weise auftreten, und so eine völlig neue Klasse von Materialien gefunden werden. Z.B. zeigt das bekannte Buckminsterfulleren C_{60} im Festkörper als *Legierung* mit Alkalimetallen supraleitende Eigenschaften mit Sprungtemperaturen bis zu 43 K [36, 37].

1.2 Dirac, Feynman und Metropolis

Spielen ist Experimentieren mit dem Zufall.

Novalis, Fragmente.

Die Pfadintegralmethode wurde 1948 von dem damals dreißigjährigen Richard P. Feynman ersonnen [5]. Angeregt hatte ihn eine *mysteriöse Bemerkung* von P.A.M. Dirac, daß die Übergangsamplitude $\langle x_2, t_2 | x_1, t_1 \rangle$ irgendwie mit dem Ausdruck

$$\exp \left[\frac{i}{\hbar} \int_{t_1}^{t_2} dt \mathcal{L}_{cl}(x, \dot{x}) \right] \quad (1.1)$$

zusammenhänge. Feynman fand, daß der gesuchte Zusammenhang einer Integration über *alle möglichen Pfade* zwischen den Raum-Zeit Punkten (x_1, t_1) und (x_N, t_N) mit 1.1 als Integranden entspricht:

$$\langle x_2, t_2 | x_1, t_1 \rangle = \int_{x_1}^{x_N} \mathcal{D}[x(t)] \exp \left[\frac{i}{\hbar} \int_{t_1}^{t_2} dt \mathcal{L}_{cl}(x, \dot{x}) \right]. \quad (1.2)$$

Das Integral in 1.2 wird durch die Diskretisierung

$$\int_{x_1}^{x_N} \mathcal{D}[x(t)] \equiv \lim_{N \rightarrow \infty} \left(\frac{m}{2\pi i \hbar \Delta t} \right)^{(N-1)/2} \int dx_{N-1} \int dx_{N-2} \dots \int dx_2, \quad (1.3)$$

$$(\Delta t = (t_N - t_1)/N) \quad (1.4)$$

dargestellt. Das Pfadintegral kann als zur Schrödinger Gleichung äquivalente Formulierung der Quantenmechanik angesehen werden. So unanschaulich 1.2 zunächst sein mag, so sehr kann dieser Ansatz bei näherer Betrachtung zum Verständnis der Quantenmechanik beitragen. In der Lagrangeschen Formulierung der klassischen Mechanik erhält man die klassischen Trajektorien über die Minimierung der klassischen Wirkung,

$$\delta \int_{t_1}^{t_2} dt \mathcal{L}_{cl}(x, \dot{x}) = 0. \quad (1.5)$$

Für quasi-klassische Systeme tragen nur die Pfade, die sehr nahe an der klassischen Trajektorie liegen, zum Pfadintegral bei. Weiter entfernt liegende Pfade

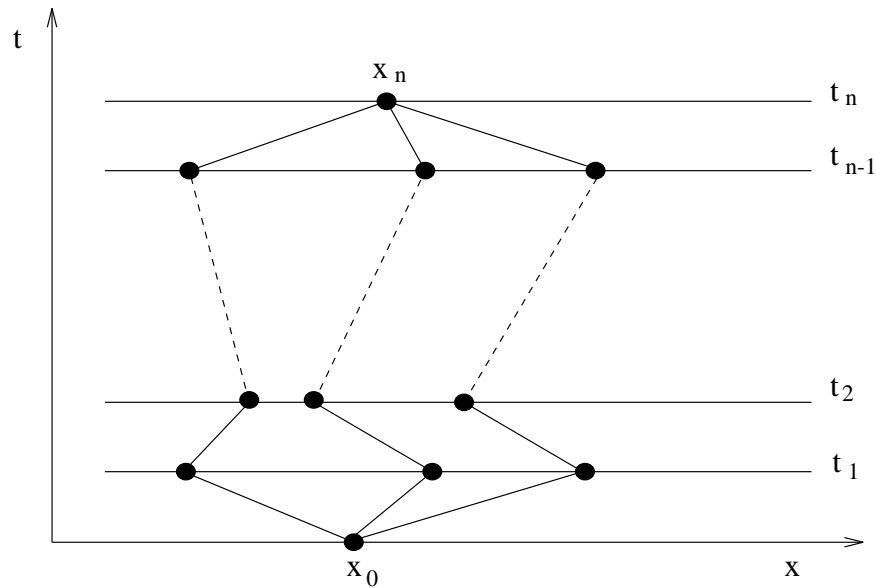


Abbildung 1.1: Pfade in der Raum-Zeit Ebene

geben wegen starker Oszillationen der Phase der Exponentialfunktion keine oder nur verschwindend kleine Beiträge.

Dies scheint die Pfadintegralmethode insbesondere für semiklassische Systeme besonders attraktiv zu machen. Tatsächlich gestaltet sich die Berechnung von 1.2 in der Praxis äußerst schwierig. Erst in den letzten Jahren wurden numerische Verfahren entwickelt, die es gestatten, bestimmte Systeme mit Hilfe des Raum-Zeit Pfadintegrals zu berechnen.

Im wesentlichen basieren die uns bekannten Methoden darauf, mit einer geeigneten Koordinatentransformation den Anteil der kinetischen Energie in 1.2 auf eine reelle Gauß-Funktion zu transformieren. Als Vorfaktor der Wirkung in 1.2 wird dazu meist eine komplexe Zeit mit der Ersetzung $it/\hbar \rightarrow \beta/2 + it/\hbar$ eingeführt (siehe z.B. [35]).

Im Gegensatz hierzu ist das thermodynamische Pfadintegral bereits an einer Vielzahl von Systemen erprobt. Viele analytische und numerische Weiterentwicklungen lassen es heute als eine etablierte und starke Methode für Anwendungen von der Quantenfeldtheorie bis zur Cluster- und Molekülphysik erscheinen.

Da wir in dieser Arbeit nur das thermodynamische Pfadintegral auf unterschiedliche Cluster anwenden, werden wir uns im folgenden ausschließlich auf dieses konzentrieren.

1.2.1 Das Thermodynamische Pfadintegral

Die thermischen Eigenschaften eines physikalischen Systems lassen sich prinzipiell vollständig durch die Dichte-Matrix ρ bzw. die Zustandssumme Z beschreiben

$$\rho(x, x') = \langle x | \exp(-\beta H) | x' \rangle \quad (1.6)$$

$$Z = \text{Tr} (\exp[-\beta H]) = \text{Tr} \rho(x, x') . \quad (1.7)$$

Ist die Dichtematrix bekannt, berechnet sich der Erwartungswert einer nur ortsabhängigen Observablen $\mathcal{X}(x)$ in einfacher Weise durch

$$\langle \mathcal{X} \rangle = \text{Tr} \frac{1}{Z} (\mathcal{X}(x, x') \rho(x, x')) . \quad (1.8)$$

Die essentielle Schwierigkeit bei der Berechnung der Dichtematrix ergibt sich daraus, daß der Hamiltonoperator H in der Regel aus zwei nicht kommutierenden Anteilen H_0 und H_1 , den Operatoren für die kinetische und die potentielle Energie besteht,

$$H_0 = \frac{\mathbf{p}^2}{2m}, \quad H_1 = V(\mathbf{x}). \quad (1.9)$$

Mit Hilfe der Trotter-Formel [7]

$$\exp(-\beta(H_0 + H_1)) = \lim_{M \rightarrow \infty} \left(\exp(-\frac{\beta}{M} H_0) \exp(-\frac{\beta}{M} H_1) \right)^M + O\left(\frac{\beta^3}{M^2}\right) \quad (1.10)$$

können die beiden Operatoranteile auseinandergezogen werden. Für die Zustandssumme Z eines Ein-Teilchen-Systems ergibt sich in Ortsdarstellung z.B.

$$\begin{aligned} Z &= \int \left[\prod_{\gamma=1}^M d\vec{x}(\gamma) \right] \prod_{\alpha=1}^M \left\{ \langle \vec{x}(\alpha) | \exp(-\frac{\beta}{M} H_0) | \vec{x}(\alpha+1) \rangle \right. \\ &\quad \left. \times \langle \vec{x}(\alpha) | \exp(-\frac{\beta}{M} H_1) | \vec{x}(\alpha) \rangle \right\} + O\left(\frac{\beta^3}{M^2}\right) \\ &= \left(\frac{Mm}{2\pi\beta\hbar^2} \right)^{(3M/2)} \int \left[\prod_{\gamma=1}^M d\vec{x}(\gamma) \right] \\ &\quad \left\{ \exp \left(- \sum_{\alpha=1}^M \frac{Mm}{2\beta\hbar^2} (\vec{x}(\alpha+1) - \vec{x}(\alpha))^2 - \frac{\beta}{M} \sum_{\alpha=1}^M V(\vec{x}(\alpha)) \right) \right\} + O\left(\frac{\beta^3}{M^2}\right) . \end{aligned} \quad (1.11)$$

Hierbei ist die periodische Randbedingung $\mathbf{x}(1) = \mathbf{x}(M+1)$ zu beachten. Der Parameter M wird in Anlehnung an das Raum-Zeit-Pfadintegral als *Anzahl der Zeitscheiben* bezeichnet, m ist die Teilchenmasse.

Der relative Fehler dieser Approximation ist sowohl von der Anzahl der Zeitscheiben als auch von β , respektive der Temperatur T , abhängig. Um Konvergenz von 1.11 innerhalb der gleichen Fehlertoleranz zu erhalten, muß die

Anzahl der Zeitscheiben in etwa proportional zu β für niedrigere Temperaturen erhöht werden.

Im Funktionallimes $M \rightarrow \infty$ ist 1.11 exakt und es ergibt sich die Feynman-Kac Formel, das thermodynamische Pfadintegral.

Für ein N-Fermionen-System müssen die N-Teilchen Zustände vollständig antisymmetrisch sein. Nach trivialer Rechnung ergibt sich z.B. für ein vollständig polarisiertes System

$$Z = \left(\frac{1}{N!}\right)^M \int \left[\prod_{\gamma=1}^M \prod_{i=1}^N d\vec{x}_i(\gamma) \right] \prod_{\delta=1}^M \det A(\delta+1, \delta) \exp\left(-\frac{\beta}{M} \sum_{\alpha=1}^M V(\vec{x}_1(\alpha), \dots, \vec{x}_N(\alpha))\right), \quad (1.12)$$

mit

$$(A(\alpha+1, \alpha))_{k,l} = \left(\frac{Mm}{2\pi\beta\hbar^2}\right)^{3/2} \exp\left(-\frac{Mm}{2\beta\hbar^2}(\vec{x}_k(\alpha+1) - \vec{x}_l(\alpha))^2\right). \quad (1.13)$$

Falls die Teilchen der Bose-Einstein Statistik unterliegen, muß die Determinante durch die entsprechende Permanente ersetzt werden.

Das zur Zeit gebräuchlichste Verfahren zur Berechnung von Pfadintegralen ist die numerische Integration mittels des Metropolis Algorithmus [6], der bereits 1953 auf einem der ersten Elektronenrechner, dem MANIAC in Los Alamos, Verwendung fand. Dieser Algorithmus basiert darauf, daß ein Markov Prozeß generiert wird, unter dem die kanonische Zustandsverteilung stationär ist.

In jedem Metropolis Schritt wird eine zufällige neue Ortskonfiguration gewählt. Der Schritt wird angenommen, falls der Absolutwert des Quotienten der neuen und alten Wichtungsfunktion, die durch die Integranden in 1.11 bzw. 1.12 gegeben ist, größer als eine Zufallszahl zwischen 0 und 1 ist. Der Erwartungswert einer beliebigen Observablen berechnet sich dann durch

$$\langle X \rangle = \frac{\sum_{s=1}^G X(s) \text{sign}(W(s))}{\sum_{s=1}^G \text{sign}(W(s))}, \quad (1.14)$$

wobei G die Anzahl der durchgeführten Metropolis Schritte ist und W(s) bzw. X(s) der Wert der Wichtungsfunktion bzw. der Observablen X im s-ten Metropolis Schritt sind. Bei diesem prinzipiell sehr einfachen Monte-Carlo Verfahren ist eine Fülle von technischen Details zu beachten. Z.B. ist die Berechnung des Erwartungswertes von Operatoren, die den Impulsoperator enthalten, nicht eindeutig. Dies ist bildlich sehr einfach zu verstehen. Durch die Diskretisierung der "Raum-Zeit"-Pfade mit einer endlichen Anzahl von Stützpunkten ergibt sich eine Reihe von verschiedenen Möglichkeiten die Ableitungen dieser Pfadfunktionen zu berechnen. Der Wert der Ableitungen hängt hierbei

ähnlich wie bei der numerischen Lösung von Differentialgleichungen davon ab, wieviele Stützpunkte in die Ableitungsberechnung eingehen und welche Spline-Funktionen den Formeln für die numerische Differentiation zugrunde liegen. Weiterhin hängt die Konvergenz des Verfahrens in hohem Maße von den Schritt-erzeugungsmechanismen, den Schrittlängen etc. ab.

Unter Ausnutzung von zur Trotter-Formel alternativer Operatoridentitäten erhält man geringfügig andere Formulierungen des Pfadintegrals, bei denen der systematische Fehler mit höheren Potenzen von M gegen 0 konvergiert ³ (siehe z.B. [9, 12]).

In unseren umfangreichen numerischen Programmen wurden diese und viele andere systematische Verbesserungen, die in den zu diesem Thema im Literaturverzeichnis angegebenen Artikeln beschrieben sind, berücksichtigt. Für Bose-Einstein- und Fermi-Dirac-Systeme wurden – wie bereits oben erwähnt – eigene systematische Verbesserungen entwickelt, die in den Kapiteln 2-4 beschrieben werden.

³Eine systematische Entwicklung erhält man beispielsweise mithilfe der Baker-Campbell-Hausdorff-Formel.

Bibliographie

□ Lehrbücher zum Thema Pfadintegral:

- [1] R.P. Feynman, A.R. Hibbs : Quantum Mechanics and Path Integrals. New York: McGraw Hill 1965
- [2] R.P. Feynman: Statistical Mechanics. Reading: Addison-Wesley 1972
- [3] H. Kleinert: Pfadintegrale. Mannheim: BI Wissenschaftsverlag 1993
- [4] M.H. Kalos, P.A. Whitlock: Monte Carlo Methods. New York: John Wiley & Sons 1986

Artikel zur Pfadintegral Monte-Carlo Methode:

- [5] R.P. Feynman, Space-Time Approach to Non-Relativistic Quantum Mechanics, Rev. Mod. Phys. **20**, 367, (1948).
- [6] N. Metropolis, A. Rosenbluth, M.N. Rosenbluth, A.H. Teller, E. Teller : Equation of State Calculations by Fast Computing Machines, J. Chem. Phys. **21**, 1087 (1953)
- [7] M.F. Trotter : Proc. Am. Math. Soc. **10**, 545 (1959)
- [8] M. Takahashi, M. Imada : Monte Carlo Calculation of Quantum Systems, J. Phys. Soc. Jpn. **53**, 963 (1984)
- [9] M. Takahashi, M. Imada : Monte Carlo Calculation of Quantum Systems. II. Higher Order Corrections, J. Phys. Soc. Jpn. **53**, 3765 (1984)
- [10] M. Imada, M. Takahashi : Quantum Monte Carlo Simulation of a Two-Dimensional Electron System - Melting of Wigner Crystal - , J. Phys. Soc. Jpn. **53**, 3770 (1984)
- [11] M. Imada : On the Monte Carlo Method for Fermions in Multidimensional Systems, J. Phys. Soc. Jpn. **53**, 2861 (1984)

- [12] M. Takahashi : Effective Potential Method in Path-Integral Monte Carlo Calculation and Application to ^4He at $T \leq 4$ K, J. Phys. Soc. Jpn. **55**, 1952 (1960)
- [13] J.D. Doll, D.L. Freeman : A Monte Carlo method for quantum Boltzmann statistical mechanics, J. Chem. Phys. **80**, 2239 (1984)
- [14] J.D. Doll, D.L. Freeman : J. Chem. Phys. **80**, 5709 (1984)
- [15] R.D. Coalson, D.L. Freeman, J.D. Doll : Partial averaging approach to Fourier coefficient path integration, J. Chem. Phys. **85**, 4567 (1986)
- [16] J.D. Doll : J. Chem. Phys. **81**, 3536 (1984)
- [17] J.D. Doll, D.L. Freeman : J. Chem. Phys. **82**, 465 (1985)
- [18] H. Kono, A. Taksaka, S.H. Lin : Monte Carlo calculation of the quantum partition function via path integral, J. Chem. Phys. **88**, 6390 (1988)
- [19] A. Giansanti, G. Jacucci: Variance and correlation length of energy estimators in Metropolis path integral Monte Carlo, J. Chem. Phys. **89**, 7454 (1988)
- [20] J. Cao, B.J. Berne: On energy estimators in path integral Monte Carlo simulations: Dependence of accuracy on algorithm, J. Chem. Phys. **91**, 6359 (1989)
- [21] E.L. Pollock, D.M. Ceperly: Simulation of quantum many-body systems by path-integral methods, Phys.Rev. **B 30**, 2555 (1984)
- [22] D.M. Ceperly, Path-Integral Calculations of Normal Liquid ^3He , Phys.Rev.Lett. **69**, 331 (1992)
- [23] P. Sindzingre, M.L. Klein, D.M. Ceperly, Path-Integral Monte Carlo Study of Low-Temperature ^4He Clusters, Phys.Rev.Lett.**63**, 1601 (1989)

Lehrbücher zur Clusterphysik:

- [24] Helmut Haberland (Editor): Clusters of Atoms and Molecules. Berlin: Springer (1994)
- [25] W. Raith [Hrsg.] : Bergmann, Schäfer - Lehrbuch der Experimentalphysik (Band 5 Vielteilchensysteme). Berlin: de Gruyter 1992

Einen guten Überblick zum Stand der Forschung in der Clusterphysik geben die Proceedings zur ISSPIC Konferenzserie:

- [26] Proceedings of the 2. International Symposium on Small Particles and Inorganic Clusters, Lausanne, Switzerland, 8-12 September 1980.
in: Surface Science **106**(1-3) (1981)
- [27] Proceedings of the 3. International Symposium on Small Particles and Inorganic Clusters (ISSPIC-3), Berlin, 9-13 July 1984.
in: Surface Science **156**
- [28] Proceedings of the 4. International Symposium on Small Particles and Inorganic Clusters, Aix-en-Provence, France, 1988.
in: Z. Phys. **D 12** (1989)
- [29] Proceedings of the 5. International Symposium on Small Particles and Inorganic Clusters, Konstanz, 16-22 September 1990.
in: Z. Phys. **D19**(1-4) (1991), *Z. Phys.* **20**(1-4)(1991)
- [30] Proceedings of the 6. International Symposium on Small Particles and Inorganic Clusters, Chicago, USA, 16-22 September 1992.
in: Z. Phys. **D26** (1993)

Weitere im Text zitierte Literatur:

- [31] G. Mie: *Ann. Phys.* **25**, 377 (1908)
- [32] G.S. Anagnostatos : Fermion/boson classification in microclusters, *Phys. Lett.* **A 157**, 65 (1991)
- [33] G.S. Anagnostatos : Alkali-atom shell modell, *Phys. Lett.* **A 154**, 169 (1991)
- [34] P.A.M. Dirac: *The Principles of Quantum Mechanics*, 2nd ed., The Clarendon Press, Oxford , (1958).
- [35] J. Chang, W.H. Miller: Monte Carlo path integration in real time via complex coordinates, *J. Chem. Phys.* **87**, 1648, (1987).
- [36] A.F. Hebard, et.al. : *Nature* **359**, 600 (1991)
- [37] K. Tanigaki, T.W. Ebbesen, S. Saito, J. Mizuki, J.S. Tsai, Y. Kubo, S. Kuroshima, *Nature* **352**, 222 (1991)

Teil 2

Teil 2

Die in den Kapiteln 2-9 abgedruckten Artikel sind im wesentlichen identisch mit den folgenden Artikeln und Vorabdrucken. Offensichtliche Druck- und sonstige Fehler wurden jedoch bereinigt.

Kapitel 2: **P. Borrmann, G. Franke:**

Recursion formulas for quantum statistical partition functions.
J.Chem.Phys 98, 2484 (1993)

Kapitel 3: **P. Borrmann:**

Path Integral Density Functional Theory.
Preprint UOL-THEO3-94-4, Universität Oldenburg (1994)

Kapitel 4: **P. Borrmann, E.R. Hilf:**

New enhancements to Feynmans Path Integral for Fermions.
Preprint UOL-THEO3-94-6, Universität Oldenburg (1994)

Kapitel 5: **P. Borrmann, D. Gloski, E.R. Hilf:**

Specific heat in the thermodynamics of clusters.
Surface Review and Letters (Zur Veröffentlichung angenommen.)

Kapitel 6: **P. Borrmann:**

How should thermodynamics for small systems be done?
Computational Materials Science 2, 593 (1994)

Kapitel 7: **P. Borrmann, B. Diekmann, E.R. Hilf, D. Tomanek:**

Magnetism of small transition metal clusters and the effects of isomerisation.
Surface Review and Letters (Zur Veröffentlichung angenommen.)

Kapitel 8: **P. Borrmann, E.R. Hilf:**

Structure and stability of polarized Li $^3\text{He}_n^+$ ions.
Z.Phys. D 26, S350 (1993)

Kapitel 9: **G.Franke, E.R. Hilf, P. Borrmann:**

The structure of small clusters: Multiple normal-modes model.
J.Chem.Phys 98, 3496 (1993)

Kapitel 2

Recursion formulas for quantum statistical partition functions

Recursion formulas for quantum statistical partition functions

Peter Borrmann

University of Bremen, Dept. of Physics, D-W2800 Bremen 33, Germany

Gert Franke

University of Oldenburg, Dept. of Physics, D-W2900 Oldenburg, Germany

Abstract

Recursion formulas are derived for Fermi-Dirac and Bose-Einstein statistical partition functions for systems where the energy can be written as a sum of one particle energies. Thus their exact partition functions can be calculated for any N .

We consider a system of N particles for which the energy can be written as a sum of one-particle energies such as ideal gases or simple shell models. We aim at a recursion of $Z(N)$ in terms of Z for subsystems. The idea may be seen as a vague analogy to cluster expansion methods.

I. THEOREM

The one-particle energy of the k -th particle being in state r_k will be denoted by $\varepsilon(r_k)$, the partition function by $Z(N)$. Then for the partition function holds

$$Z(N) = \frac{1}{N} \sum_{k=1}^N (\pm 1)^{k+1} S(k) Z(N-k) \quad (1)$$

with $Z(0) = 1$ and $S(k)$, which can be identified as the Boltzmannian partition function of a cluster of size k , given by

$$S(k) := \sum_j \exp(-\beta k \varepsilon(j)) . \quad (2)$$

The minus and the plus signs stand for Fermi-Dirac and Bose-Einstein statistics, respectively. The sum in (2) runs over all possible states.

II. PROOF

A. Fermi Dirac statistics

In the case of Fermi-Dirac statistics the partition function may be written as ¹:

$$Z_{\text{FD}}(N) = \frac{1}{N!} \sum_{r_1} \sum_{r_2 \neq r_1} \dots \sum_{r_N \neq r_1, r_2, \dots, r_{N-1}} \exp\left(-\beta \sum_{k=1}^N \varepsilon(r_k)\right) . \quad (3)$$

Splitting the inner sum into two terms gives

$$Z_{\text{FD}}(N) = \frac{1}{N} \left[\frac{1}{(N-1)!} \sum_{r_1} \sum_{r_2 \neq r_1} \dots \sum_{r_{N-1} \neq r_1, r_2, \dots, r_{N-2}} \exp\left(-\beta \sum_{k=1}^{N-1} \varepsilon(r_k)\right) \right] * \quad (4)$$

$$* \left\{ \sum_{r_N} \exp(-\beta \varepsilon(r_N)) - \sum_{j=1}^{A-1} \exp(-\beta \varepsilon(r_j)) \right\} .$$

The term in square brackets is just $Z_{\text{FD}}(N-1)$, the first term in the curly brackets is $S(1)$. Thus equation (4) takes the form

$$Z_{\text{FD}}(N) = \frac{1}{N} S(1) Z_{\text{FD}}(N-1) - \frac{1}{N!} \sum_{j=1}^{N-1} \left\{ \sum_{r_1} \sum_{r_2 \neq r_1} \dots \sum_{r_{N-1} \neq r_1, r_2, \dots, r_{N-2}} \exp\left(-\beta \sum_{k=1}^{N-1} \varepsilon(r_k)\right) \exp(-\beta \varepsilon(r_j)) \right\} .$$

Because of permutational symmetry the term in the brackets is independent of j . Hence the outer sum gives simply a factor $(N-1)$ and j can be chosen arbitrarily.

$$\begin{aligned}
 Z_{\text{FD}}(N) &= \frac{1}{N} S(1) Z_{\text{FD}}(N-1) - \\
 &\quad - \frac{N-1}{N!} \sum_{r_1} \sum_{r_2 \neq r_1} \dots \sum_{r_{N-1} \neq r_1, r_2, \dots, r_{N-2}} \exp\left(-\beta \sum_{k=1}^{N-2} \varepsilon(r_k)\right) \exp(-2\beta \varepsilon(r_{N-1})) \\
 &= \frac{1}{N} S(1) Z_{\text{FD}}(N-1) - \frac{1}{N} S(2) Z_{\text{FD}}(N-2) + \frac{(N-1)(N-2)}{N!} * \\
 &\quad * \sum_{r_1} \sum_{r_2 \neq r_1} \dots \sum_{r_{N-2} \neq r_1, r_2, \dots, r_{N-3}} \exp\left(-\beta \sum_{k=1}^{N-3} \varepsilon(r_k)\right) \exp(-3\beta \varepsilon(r_{N-3})).
 \end{aligned}$$

Repeated use of these transformations yields equation (1).

q.e.d.

B. Bose-Einstein statistics

For bosons the partition function takes the form ¹:

$$Z_{\text{BE}}(N) = \sum_{r_1, r_2, \dots, r_N} g(r_1, r_2, \dots, r_N) \exp\left(-\beta \sum_{k=1}^N \varepsilon(r_k)\right) \quad (5)$$

where g is

$$g(r_1, r_2, \dots, r_N) = \frac{1}{N!} \prod_{k=0} N_k!$$

and N_k being the number of particles in state k .

Using the definition of g in a recursive way

$$g(r_1, r_2, \dots, r_N) = \frac{1}{N} g(r_1, \dots, r_{N-1}) \left(1 + \sum_{j=1}^{N-1} \delta_{r_j, r_N}\right)$$

and dividing the sums in (5) into two parts gives

$$\begin{aligned}
 Z_{\text{BE}}(N) &= \sum_{r_1, r_2, \dots, r_{N-1}} g(r_1, r_2, \dots, r_{N-1}) \exp\left(-\beta \sum_{k=1}^{N-1} \varepsilon(r_k)\right) * \\
 &\quad \sum_{r_N} \frac{1}{N} \left(1 + \sum_{j=1}^{N-1} \delta_{r_j, r_N}\right) \exp(-\beta \varepsilon(r_N)) \\
 &= \frac{1}{N} S(1) Z_{\text{BE}}(N-1) + \frac{1}{N} \sum_{j=1}^{N-1} \sum_{r_1, r_2, \dots, r_{N-1}} g(r_1, r_2, \dots, r_{N-1}) * \\
 &\quad * \exp\left(-\beta \sum_{k=1}^{N-1} \varepsilon(r_k)\right) \exp(-\beta \varepsilon(r_j)).
 \end{aligned}$$

In the second step again advantage has been taken of the permutational symmetries. Proceeding in the same manner as above for Fermi Dirac statistics yields the theorem. **q.e.d.**

III. CONCLUSIONS

The recursion formula given in the theorem is exact. For practical purposes the sums may be done only over finite number of states which yields a good approximation up to temperatures where the occupation numbers of higher states are sufficiently small. Using the derived recursion formulas for the partition functions the computational effort increases approximately with the number n_{\max} of states taken into account for the functions $S(k)$, ($k = 1, \dots, N$), and with the square of the particle number for equation (1). In contrast, the numerical effort to evaluate the usual equations (3) and (5) directly, increases roughly with $(n_{\max})^N$.

The given recursion formulas may be applied in cluster physics as well as in the framework of simple models in nuclear physics. Recently, Mendel² applied our results in a special model of Quantum Chromo dynamics.

ACKNOWLEDGMENTS

We thank E.R.Hilf for fruitful discussions.

REFERENCES

- ¹ Reif, F. : Fundamentals of statistical and thermal physics, Singapore: McGraw-Hill 1965
- ² E. Mendel : preprint, Universität Oldenburg, 1992

Kapitel 3

Path Integral Density Functional Theory

Path Integral Density Functional Theory

Peter Borrmann

Department of Physics, Carl von Ossietzky Universität Oldenburg, D-26111

Oldenburg, Germany

Abstract

A new method (PI-DFT) which combines path integrals and density functional theory is proposed as a pathway to many fields of physics. Within path integral theory it is possible to construct particle densities without explicitly calculating individual wave functions. These densities can directly be used as an input to energy density functionals. Thus our method makes full use of the theorem of Hohenberg, Kohn and Sham, which shows that the energy of a many electron system only depends on the particle density.

At glance we present a recursion formula for the calculation of many fermion and boson particle densities from one-particle densities at a set of different temperatures. For both statistics the numerical effort of our method increases only with the square of the particle number.

Path integrals and Density Functional Theory have both been investigated and developed extensively in the past decades ¹. Here we present a new method (PI-DFT), which formally joins both fields and for the first time uses the theorem of Hohenberg, Kohn and Sham [3,4] to its full extent. While the method is applicable to bosons as well, the most interesting case is that of fermions because of its great relevance in quantum chemistry. The pride of our method is that we never deal with individual wave functions to compute the particle densities but still solve the full problem. The basic underlying idea is a self-consistent iteration scheme, in which the particle density is computed by means of path integrals, while effective potentials and observables are computed with methods lent from density functional theory.

For the problem of constructing completely antisymmetric or symmetric particle densities we propose a recursion formula which has originally been invented by us for the partition function [5]. With this formula there is no need to know the individual wave functions to construct the appropriate particle densities for Fermi-Dirac (FD) or Bose-Einstein (BE) statistics. Instead, these are calculated from single-particle densities but at different temperatures.

Using this formula the numerical effort for both statistics grows only with the square of the particle number.

In the following we will consider N-particle hamiltonians of the form

$$H = -\frac{\hbar^2}{2m} \sum_{i=1}^N \frac{d^2}{dx_i^2} + \sum_{i=1}^N v(\vec{x}_i) + \sum_{k<l}^N u(|\vec{x}_k - \vec{x}_l|) . \quad (1)$$

That is, we assume the potential to contain one and two particle interaction terms as encountered typically in quantum chemical problems.

In conventional Path Integral Monte Carlo techniques for fermion systems

¹See for example [1,2] and references therein.

an NM dimensional integral with an integrand containing an $(N \times N)$ determinant has to be calculated (see e.g. [6,7]) resulting in a numerical effort proportional to N^4 . Equation (2) can be derived easily using the Trotter formula [8] and is equivalent to the thermal Path Integral as the number of *time slices* M goes to infinity.

$$Z = \left(\frac{1}{N!} \right)^M \int \left[\prod_{k=1}^N \prod_{\mu=1}^M d\vec{x}_k(\mu) \right] \prod_{\nu=1}^M \left\{ \det A(\nu) \times \exp \left(-\frac{\beta}{M} \left[\sum_{k=1}^N v(\vec{x}_k(\nu)) + \sum_{k<l}^N u(|\vec{x}_k(\nu) - \vec{x}_l(\nu)|) \right] \right) \right\} \quad (2)$$

with

$$(A(\mu))_{k,l} = \left(\frac{Mm}{2\pi\beta\hbar^2} \right)^{3/2} \exp \left(-\frac{Mm}{2\beta\hbar^2} (\vec{x}_k(\mu) - \vec{x}_l(\mu+1))^2 \right),$$

$$\vec{x}_k(M+1) \equiv \vec{x}_k(1).$$

Although the method is suitable for systems like ${}^3\text{He}$ clusters [9] and most physical relevant observables can be calculated, its application is numerically very extensive in general.

According to the theorem of Hohenberg, Kohn and Sham [3,4] and its extension to thermal systems given by Mermin [10] the potential given by the term in square brackets in (2) can be replaced by an effective one-particle potential

$$\varphi(\vec{x}) = v(\vec{x}) + \int d\vec{x}' \eta(\vec{x}') u(|\vec{x}' - \vec{x}|). \quad (3)$$

Since the energy is only a functional of the one particle density $\eta(\vec{x})$, which can be easily calculated within the approximation (2) by Monte Carlo methods and $\varphi(\vec{x}')$, the solution of the stated problem can be found by self-consistent iteration of (2) and (3). A priori the use of this approximation has no advantages compared to the direct calculation of (2), but together with a much more

effective way of calculating the partition function, which will be stated in the following, the above iteration scheme develops to a very powerful tool.

Let us denote with $\eta_N(\vec{x}; \beta)$ the probability of finding a particle at position \vec{x} in a system of N noninteracting fermions or bosons moving in a common potential thermalized at temperature β and with $Z_N(\beta)$ the corresponding canonical partition function. For such a system it is sufficient to compute the one-particle densities $\eta_1(\vec{x}; \beta), \eta_1(\vec{x}; 2\beta), \dots, \eta_1(\vec{x}; N\beta)$, but at a set of different temperatures. Then $Z_N(\beta)$ and $\eta_N(\vec{x}, \beta)$ can be calculated by the recursion formulas

$$Z_N(\beta) = \frac{1}{N} \sum_{k=1}^N (\pm)^{k+1} Z_1(k\beta) Z_{N-k}(\beta) \quad (4)$$

$$\eta_N(\vec{x}; \beta) = Z_N^{-1}(\beta) \sum_{k=1}^N (\pm)^{k+1} Z_1(k\beta) \eta_1(\vec{x}, k\beta) Z_{N-k}(\beta) \quad (5)$$

where the plus and the minus signs stand for Fermi-Dirac and Bose-Einstein statistics, respectively, and $Z_0(\beta) \equiv 1$.

The proof for (4) has already been given explicitly in [5]. The validity of (5) can be proven in the same manner. As the whole procedure is somewhat lengthy, we omit it here and sketch the basic idea using the two-fermion system as an example.

Let ϵ_k denote the energy eigenvalues of the one-particle system and ψ_k the corresponding eigenfunctions. Then the partition function is given by

$$Z_2(\beta) = \frac{1}{2} \sum_k \sum_{l \neq k} \exp(-\beta(\epsilon_k + \epsilon_l)) . \quad (6)$$

The probability p_k of finding a particle in the one-particle state $|k\rangle$ is simply

$$\begin{aligned} p_k &= Z_2^{-1}(\beta) \frac{1}{2} \sum_{l \neq k} \exp(-\beta(\epsilon_k + \epsilon_l)) \\ &= Z_2^{-1}(\beta) \frac{1}{2} \sum_l \exp(-\beta(\epsilon_k + \epsilon_l)) - \exp(-2\beta\epsilon_k) \\ &= Z_2^{-1}(\beta) \frac{1}{2} [\exp(-\beta\epsilon_k) Z_1(\beta) - \exp(-2\beta\epsilon_k)] \end{aligned} \quad (7)$$

For the particle density this yields

$$\begin{aligned}
 \eta_2(\vec{x}; \beta) &= \sum_k p_k |\psi_k(\vec{x})|^2 \\
 &= Z_2^{-1}(\beta) \sum_k |\psi_k(\vec{x})|^2 [\exp(-\beta\epsilon_k) Z_1(\beta) - \exp(-2\beta\epsilon_k)] \\
 &= Z_2^{-1}(\beta) [Z_1^2(\beta) \eta_1(\vec{x}; \beta) - Z_1(2\beta) \eta_1(\vec{x}; 2\beta)] ,
 \end{aligned} \tag{8}$$

which is nothing but equation (5) for the special case $N = 2$.

A simple example shows that the given formulas work very well and exactly.

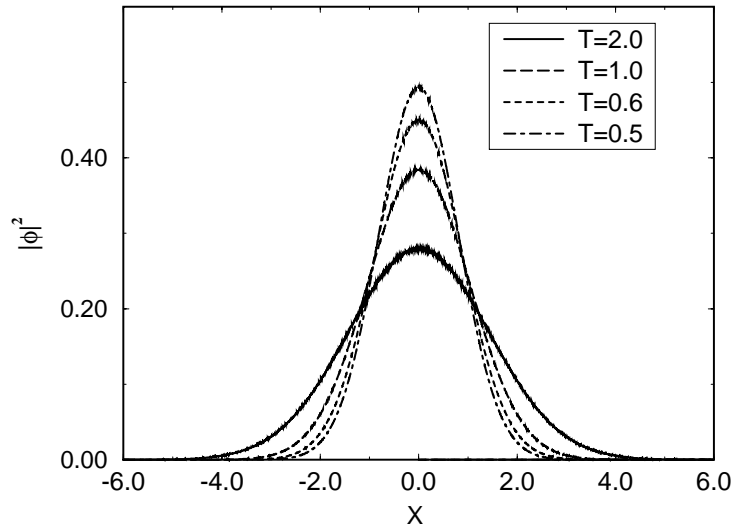


FIG. 1. Particle densities $\eta_1(\vec{x}; \beta)$ calculated with Path Integral Monte Carlo for various temperatures ($\hbar = k = m = 1$).

We calculated the exact solvable system of N uncoupled harmonic oscillators

$$H = -\frac{\hbar^2}{2m} \sum_k \frac{d^2}{dx_k^2} + \frac{1}{2} x_k^2 \tag{9}$$

for both statistics. The one particle densities $\eta_1(\vec{x}; k\beta)$ shown in Fig. 1 are calculated with standard path integral techniques (see e.g. [6,7]). In Fig. 2 and Fig. 3 the exact particle densities and the densities calculated via (5) are shown for both statistics. The outcome is an almost perfect agreement with the exact results. The computed energies agree equally well with the exact values. For our examples the errors were in all cases below 0.1 %.

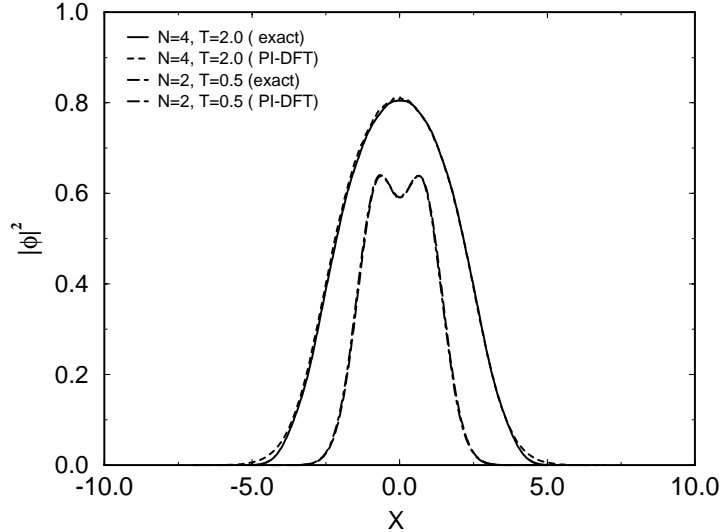


FIG. 2. Exact harmonic oscillator particle densities and particle densities calculated with Path Integral Monte Carlo in connection with equation (3) for $N=2$ at $T=0.5$ and $N=4$ at $T=2.0$ for the case of FD statistics ($\hbar = k = m = 1$).

Obviously it is essential in the fermion case, that there is a nonvanishing occupation probability of the excited states for the chosen temperature, i.e. the results of the one-particle Path Integral Monte Carlo simulations have to contain information about the excited states. Because of the fact that in the low temperature range the energy is in general a very slowly increasing function in the case of Fermi-Dirac statistics, this is not a too bad restriction, even if one is going to calculate ground state properties of the fermion system.

Possibly the most interesting topic concerning PI-DFT is an analysis of its computational costs. The basic steps in PI-DFT are the following:

1. Construction of an initial guess for the N particle density.
2. Calculation of the effective potential.
3. Calculation of single-particle densities and the corresponding energies at N different temperatures.

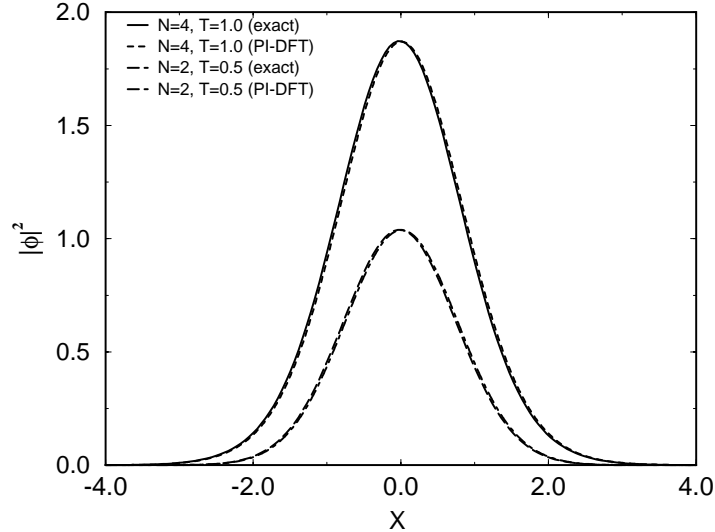


FIG. 3. Exact harmonic oscillator particle densities and particle densities calculated with Path Integral Monte Carlo in connection with equation (3) for $N=2$ at $T=0.5$ and $N=4$ at $T=1.0$ for the case of BE statistics ($\hbar = k = m = 1$).

4. Calculation of the partition function by spline interpolation of the caloric curve along with numerical integration using

$$Z(\beta) = \exp\left(-\int_{\beta_0}^{\beta} d\beta' E(\beta') + F_0\right). \quad (10)$$

5. Calculation of the N -particle partition function using (4).
6. Calculation of the N -particle density using (5).

Steps 2-6 have to be repeated until the particle densities and the energy are converged. The main numerical effort lies in the steps 2 and 3. The calculation of the effective potential is usually proportional to N^2 . Because of the fact that the numerical effort of a Path Integral Monte Carlo simulation grows normally proportionally to β the same applies to step 3. Steps 4 and 5 are negligible, while the effort for step 6 again grows proportionally to N^2 assuming that the number of used grid points is approximately proportional to the number of particles. Overall this indeed yields a numerical effort proportional to the

square of the particle number for PI-DFT. Hence it follows that PI-DFT can be seen as a formal proof, that e.g. quantum chemical calculations can be done with such a slowly increasing numerical effort. We hope that this will encourage further improvements of other related methods, too. This paper presents only the onset of PI-DFT and a lot of improvements seem to be possible and required. For example, the recursion for the partition function might be numerically unstable under unfavorable circumstances in the case of FD statistics because of the alternating sums.

In a forthcoming paper we will present a study on ^4He clusters as a first physical application of PI-DFT.

ACKNOWLEDGMENTS

We wish to thank E.R. Hilf for very fruitful and helpful discussions.

REFERENCES

- [1] R.O. Jones, O. Gunnarsson: *Rev. Mod. Phys.* **61**, 689 (1989)
- [2] H. Kleinert: *Pfadintegrale*, BI Wissenschaftsverlag, Mannheim 1993
- [3] P. Hohenberg, W. Kohn: *Phys. Rev.* **136** (3B), B864 (1964)
- [4] W. Kohn, L.J. Sham: *Phys. Rev.* **140** (4A), A1153 (1965)
- [5] P. Borrmann, G. Franke: *J. Chem. Phys.* **98**, 2484 (1993)
- [6] M. Takahashi, M. Imada : *J. Phys. Soc. Jpn.* **53**, 963 (1984)
- [7] M. Takahashi, M. Imada : *J. Phys. Soc. Jpn.* **53**, 3765 (1984)
- [8] M.F. Trotter : *Proc. Am. Math. Soc.* **10**, 545 (1959)
- [9] P. Borrmann, E.R. Hilf: *Z.Phys.* **D 26** , S350 (1993)
- [10] N.D. Mermin: *Phys. Rev.* **137** (5A), A1441 (1965)

Kapitel 4

New enhancements to Feynmans Path Integral for fermions

New enhancements to Feynmans Path Integral for fermions

Peter Borrmann, Eberhard R. Hilf

Department of Physics, University of Oldenburg, D-26111 Oldenburg, Germany

Abstract

We show that the computational effort for the numerical solution of fermionic quantum systems, occurring e.g., in quantum chemistry, solid state physics, field theory in principle grows with less than the square of the particle number for problems stated in one space dimension and with less than the cube of the particle number for problems stated in three space dimensions. This is proven by representation of effective algorithms for fermion systems in the framework of the Feynman Path Integral.

I. INTRODUCTION

When Feynman stated the thermodynamical Path Integral for fermions (see [1] and references therein), he was in doubt whether this formula could ever be used in numerical applications. However, in the last few years considerable progress has been made in the development of Path Integral Monte Carlo algorithms. Especially D. Ceperly et. al. [2] proposed many very useful refinements. Nevertheless, the problem of applying Path Integral methods to fermion systems remains hard to be solved. The reasons are the so-called fermion sign problem and the computational effort, which grows normally proportional to the fourth power of the number of particles N . In this letter we

present a formally exact method with a computational effort growing only with the cube of the particle number.

We further show, that there are some strong indications, that the computational effort should in general grow only with the square of the particle number.

For problems stated in one space dimension, we give an explicit proof for that.

II. EFFECTIVE PATH INTEGRAL METHOD

A quantum N body system in thermal equilibrium can be described completely by the quantum partition function

$$Z = \text{Tr} \exp(-\beta(H_0 + H_1)) , \quad (1)$$

where H_0 and H_1 are the kinetic and potential energy operator. The Path Integral formalism leads to a computational convenient equation to calculate Z . Using Trotter's formula [3] Z can be approximated by

$$Z = \text{Tr} \left(\exp(-\frac{\beta}{M}H_0) \exp(-\frac{\beta}{M}H_1) \right)^M + O(\beta^3/M^2). \quad (2)$$

For a system of polarized fermions in d space dimensions this leads to the dNM dimensional integral:

$$Z = \left(\frac{1}{N!} \right)^M \int \left[\prod_{\gamma=1}^M \prod_{i=1}^N d\vec{x}_i(\gamma) \right] \prod_{\delta=1}^M \det A(\delta + 1, \delta) \exp \left(-\frac{\beta}{M} \sum_{\alpha=1}^M V(\vec{x}_1(\alpha), \dots, \vec{x}_N(\alpha)) \right) , \quad (3)$$

with

$$(A(\alpha + 1, \alpha))_{k,l} = \left(\frac{Mm}{2\pi\beta\hbar^2} \right)^{d/2} \exp(-\frac{Mm}{2\beta\hbar^2}(\vec{x}_k(\alpha + 1) - \vec{x}_l(\alpha))^2), \quad (4)$$

and the periodicity condition $\vec{x}_i(M + 1) = \vec{x}_i(1)$. The particle mass is denoted by m .

A number of useful modifications to (3), which improve the convergence vs.

the number of timesteps M (see e.g. [4,5]), are known. Because these modifications do not affect any of the following we will not stress them here.

Usually the Metropolis algorithm [6] is adopted to evaluate (3). The improvements presented in this paper are based on a careful analysis of the numerical algorithms.

Within the Metropolis Monte Carlo procedure a Markov process has to be generated, under which the probability distribution is stationary. In our case this condition is fulfilled by the following widely used procedure, in which the sampling of the probability distribution is done by generating two different types of random moves of the particle coordinates.

In every microscopic step, all time slices of all particle coordinates are moved separately through

$$\vec{x}_i(\alpha) \rightarrow \vec{x}_i(\alpha) + \Delta\vec{x}, \quad (5)$$

where $\Delta\vec{x}$ is a randomly chosen vector. In every macroscopic step all time slices of every particle coordinate are moved at once by constant vector.

$$\vec{x}_i(\alpha) \rightarrow \vec{x}_i(\alpha) + \Delta\vec{y}, \quad \alpha = 1 \dots M. \quad (6)$$

In both cases a move is accepted, if the absolute value of the ratio of weight functions, which are simply the integrands in (3), is greater than a homogeneous random number. Here it is important that the absolute values have to be taken, because the determinant occurring in the weight function $W(p)$ becomes sometimes negative.

Any observable X can then be evaluated through

$$\langle X \rangle = \frac{\sum_{p=1}^G X(p) \text{sign}(W(p))}{\sum_{p=1}^G \text{sign}(W(p))} \quad (7)$$

where the summation in (7) runs over all Metropolis steps, $X(p)$ being the

value of X in the p -th step.

Albeit the fact, that this method has been applied in some cases (see e.g. [7]), its usefulness is limited by its high computational costs. The main effort in the numerical computation of (3) is the calculation of the determinant. In every complete microscopic motion the determinant has to be calculated $N \times M$ times. The complete algorithm is therefore of order $\leq N^4$, if standard matrix factorizations, which are of order N^3 , are used. The lower sign stands, because we found that the number of iterations necessary to achieve a given precision in the numerical solution decreases with an increasing number of particles. This results simply from the fact that a larger number of identical particles yields better statistics.

Now observe, that every change of a microscopic coordinate affects only the i 'th row of matrix $A(\alpha + 1, \alpha)$ and the i 'th column of matrix $A(\alpha, \alpha - 1)$. This simple fact can be used to reduce the numerical effort by a factor n . The reason for that is that the updating of an LU factorization of a matrix after a row or column exchange can be done by a numerical effort proportional to N^2 . Descriptions of such algorithms can be found in some textbooks on matrix computations [8]. We thus claim that the total algorithm is only of order N^3 . Encouraged by the above result and through the fact that the matrix (4) has some hidden symmetries having only $2dN$ independent parameters instead of N^2 , we found for the special case of systems describable in one space dimension ($d = 1$) a further reduction of the numerical effort.

Absorbing the trivial constant factors in (4) the problem is reduced to calculate the determinant of matrices of the form

$$B_{i,j} = \exp\left(-\frac{1}{2}(x_i - y_j)^2\right). \quad (8)$$

Using the linear properties of \det we have

$$\det(B) = \det(M) \prod_{j=1}^N \exp\left(-\frac{1}{2}(x_j^2 + y_j^2)\right). \quad (9)$$

We now show, that the determinant of matrices of the special form

$$M_{i,j} = \exp(x_i y_j) \quad (10)$$

can be calculated with an effort of only N^2 operations. This can most easily be seen using the decomposition $M = RS^{-1}T$ of (10).

$$R = \begin{pmatrix} 1 & y_1 & y_1^2 & \cdots \\ 1 & y_2 & y_2^2 & \cdots \\ \vdots & \vdots & \vdots & \vdots \\ 1 & y_N & y_N^2 & \cdots \end{pmatrix}, S = \begin{pmatrix} 0! & 0 & 0 & \cdots \\ 0 & 1! & 0 & \cdots \\ 0 & 0 & 2! & \cdots \\ \vdots & \vdots & \vdots & \ddots \end{pmatrix}, T = \begin{pmatrix} 1 & 1 & \cdots & 1 \\ x_1 & x_2 & \cdots & x_N \\ x_1^2 & x_2^2 & \cdots & x_N^2 \\ \vdots & \vdots & \vdots & \vdots \end{pmatrix}. \quad (11)$$

The truncation of these infinite matrices to simple $(N \times N)$ -matrices corresponds to a truncation of the exponential series at order $N - 1$. For sufficiently large N there is obviously no problem in doing so and we have

$$\det(M) = \det(R) \det(S) \det(T). \quad (12)$$

The calculation of $\det(S)$ is just trivial and yields a constant for given N . R and T are Vandermonde matrices, for which the calculation of the determinants is extremely simple [9]. For example for R we have

$$\det(R) = \prod_{1 \leq j < i \leq N} (x_i - x_j). \quad (13)$$

The complete calculation of $\det M$ thus involves $N(N - 1)$ subtractions and $N(N - 1)$ multiplications altogether. Again using the fact, that only one coordinate is changed in one microscopic step, the algorithm to compute the determinant is of order N and the complete Monte Carlo algorithm thus of order N^2 .

Thus we are able to rewrite (3) as

$$\begin{aligned}
Z = & \left(\frac{1}{N!}\right)^M \left(\frac{Mm}{2\pi\beta\hbar^2}\right)^{NM/2} \left(\prod_{i=1}^N \frac{1}{i!}\right) \int \prod_{\alpha=1}^M \prod_{i=1}^N dx_i(\alpha) \exp\left(-\frac{Mm}{\beta\hbar^2} \sum_{\alpha=1}^M \sum_{j=1}^N x_j^2(\alpha)\right) \quad (14) \\
& \left(\frac{Mm}{\beta\hbar^2}\right)^{NM} \left(\prod_{\alpha=1}^M \prod_{l<k}^N (x_k(\alpha+1) - x_l(\alpha))^2\right) \exp\left(-\frac{\beta}{M} \sum_{\alpha=1}^M V(\vec{x}_1(\alpha), \dots, \vec{x}_N(\alpha))\right).
\end{aligned}$$

III. CONCLUSION

Our almost trivial looking results based on basic linear algebra contribute a significant improvement to the Path Integral method. The decomposition of (10) found together with the truncation of the indefinite matrices is somewhat unsatisfactory, because the method applies in principle only to large particle numbers. Nonetheless, our results should be encouraging to continue to look for efficient algorithms to compute the determinant of (10).

Because of the equivalence of the mathematical problem, quite generally our result implies that any solution method for quantum systems involving fermions should be bound by a computational effort of order N^2 .

Indeed, a completely different method of computing the Path Integral for N fermion and boson systems was found, which has this property [10,11].

REFERENCES

- [1] R.P. Feynman, A.R. Hibbs : Quantum Mechanics and Path Integrals New York: McGraw Hill 1965
- [2] D.M. Ceperly, Phys.Rev.Lett. **69**, 331 (1992)
E.L. Pollock, D.M. Ceperly, Phys.Rev. **B 30**, 2555 (1984)
E.L. Pollock, D.M. Ceperly, Phys.Rev. **B 36**, 8343 (1987)
- [3] M.F. Trotter , Proc. Am. Math. Soc. **10**, 545 (1959)
- [4] M. Takahashi, M. Imada , J. Phys. Soc. Jpn. **53**, 963 (1984)
- [5] M. Takahashi, M. Imada , J. Phys. Soc. Jpn. **53**, 3765 (1984)
- [6] N. Metropolis, A. Rosenbluth, M.N. Rosenbluth, A.H. Teller, E. Teller , J. Chem. Phys. **21**, 1087 (1953)
- [7] P. Borrmann, E.R. Hilf, Z.Phys.**D 26**, S350 (1993)
- [8] G.H. Golub, C.F. Van Loan, Matrix Computations, The John Hopkins University Press, Baltimore, Maryland, 1989.
J.W. Daniel, W.B. Gragg, L. Kaufmann, G.W. Stewart, Mathematics of Computation **30** 772 (1976)
P.E. Gill, G.H. Golub, M. Murray, M.A. Saunders, Mathematics of Computation **28** 772 (1976)
- [9] R. Bellmann, Introduction to Matrix Analysis, 2nd edition, New Dehli: Tata McGraw-Hill 1979 (pg. 193)
- [10] P. Borrmann, G.Franke, J.Chem.Phys.**98** 2484 (1993)
- [11] P. Borrmann, Path Integral Density Functional Theory, Preprint UOL-THEO3-94-4, Universität Oldenburg, 1994.

Kapitel 5

Specific heat in the thermodynamics of clusters

Specific heat in the thermodynamics of clusters

Peter Borrmann, Dorian Gloski, Eberhard R. Hilf

Department of Physics, Carl v. Ossietzky University Oldenburg,

D-26111 Oldenburg, Germany

Abstract

The thermodynamic properties such as the specific heat are uniquely determined by the second moments of the energy distribution for a given ensemble averaging. However for small particle numbers the results depend on the ensemble chosen. We calculated the higher moments of the distributions of some observables for both the canonical and the microcanonical ensemble of the same van der Waals clusters. The differences of the resulting thermodynamic observables for the two ensembles are calculated in terms of the higher moments. We demonstrate how for increasing particle number these terms decrease to vanish for bulk material.

For the calculation of the specific heat within the microcanonical ensemble we give a new method based on an analysis of histograms.

I. INTRODUCTION

Van der Waals clusters have been investigated both with microcanonical and canonical simulation methods in the past (see [4–6,9] and references therein). While canonical simulations are done almost exclusively with the Metropolis algorithm [12], for microcanonical simulations there are the alternatives of doing them by molecular dynamics or with the Creutz algorithm

[7,11].

The main interest in most publications so far lies on the identification and classification of phase transitions in van der Waals clusters. The deficiencies of all simulation methods mentioned above occur in the region of the so-called *Berry phase*. The reason for that is the large number of isomers which has to be taken into account for a correct calculation of the partition function [5].

Albeit the fact, that we use for the reason of good comparability Argon clusters as our test system, in this work we will not be concerned with the questions mentioned above. Instead our main interest here lies in the dependence of the higher moments of the statistical distribution functions on the particle number and the differences between microcanonical and canonical descriptions. It is well known that for the case of the canonical ensemble both the internal energy $\langle E \rangle$ and the constant volume heat capacity $C_V = \frac{1}{k_B T^2} \langle (E - \langle E \rangle)^2 \rangle$ are approximately proportional to the number of degrees of freedom (see e.g. [3]). This immediately sets up that the relative fluctuations in energy become smaller as the system size increases

$$\Delta_R E \equiv \sqrt{\langle (E - \langle E \rangle)^2 \rangle} / \langle E \rangle \sim N^{-1/2} \quad (1)$$

Indeed one might see this as the *reason* for the existence of the Berry phase and one expects that its temperature width should decrease with increasing particle number.

The higher moments of state variables are normally not of much interest in thermodynamics. The reason is that they can easily be calculated by means of the dissipation-fluctuation theorem from the first moments. For small systems, however, higher moments are a unique tool to sensitively study the subtle differences of the same thermodynamic quantity from partition functions of different ensembles, since the higher moments explore more sensitively the

form of the distribution (see [1,2]).

The van der Waals clusters explored here are an extremely simple example because only one independent variable is to be given, while the volume, the surface and so on adjust themselves.

II. COMPUTATIONAL METHOD

A system of Ar_n clusters is modelled with the usual Lennard-Jones Potential for the interatomic binding,

$$v(r) = 4\varepsilon \left(\left(\frac{\sigma}{r} \right)^{12} - \left(\frac{\sigma}{r} \right)^6 \right) \quad (2)$$

with parameters $\varepsilon = 10.3\text{meV}$ and $\sigma = 3.405\text{\AA}$.

A. Canonical Monte Carlo

For the canonical ensemble the partition function

$$Z = \int \prod_{i=1}^N d\vec{x}_i \exp(-\beta V(\vec{x}_1, \dots, \vec{x}_n)) \quad (3)$$

is calculated using the well known Metropolis [12] Monte Carlo algorithm. For optimal performance we use for the calculation of all thermodynamic quantities the histogram method of Ferrenberg et al. [13,14,5]. For convenience we give a short outline of the procedure.

If we perform R Metropolis simulations at parameters β_i and store the Monte Carlo data as histograms $N_\beta(E)$ with n_{β_i} being the total number of observations in the i 'th run, the probability distribution is given through

$$P_\beta(E) = N_\beta(E)/n_\beta = W(E) \exp(-\beta E + \beta F), \quad (4)$$

where $W(E)$ is the density of states, and F is the Helmholtz free energy. Following Ferrenberg et al. the normalized probability distribution can be improved by

$$D_\beta(E) = \frac{\sum_{i=1}^R N_i(E)}{\sum_{i=1}^R n_i \exp(-(\beta_i - \beta)E + \beta F_i)} \quad (5)$$

where

$$\sum_E D_{\beta_i} = \exp(\beta F_i), \quad (6)$$

which is simply the partition function. The values of F_i can be determined within an additive by selfconsistent iteration of (5) and (6). Simply spoken, this method improves $D_\beta(E)$ by use of simulation data at other histogram data weighted by the number of observations. We slightly improved the method by using fitted probability distributions which are sacrificed by χ^2 tests.

Now the mean value of any observable $O(E)$ can be calculated easily as a function of β .

$$\langle O_\beta(E) \rangle = \frac{1}{Z_\beta} \int_E O(E) D_\beta(E) . \quad (7)$$

B. Microcanonical Monte Carlo

The microcanonical partition function

$$Z = \int \prod_{i=1}^n d\vec{x}_i \prod_{j=1}^n d\vec{p}_j \delta[H(\vec{x}_1, \dots, \vec{x}_n, \vec{p}_1, \dots, \vec{p}_n) - E] \quad (8)$$

is approximated with the microcanonical Monte Carlo algorithm invented by Creutz [7,11,10]. The algorithm simulates the integral

$$Z = \int \prod_{i=1}^n d\vec{x}_i \int_0^{E-V_0} dE_D \delta[V(\vec{x}_1, \dots, \vec{x}_n) + E_D - E]. \quad (9)$$

where V_0 is the minimal potential energy, in our case the potential energy of the *best single cluster* configuration. E_D is an extra degree of freedom called demon, which simulates the kinetic energy of the system and is restricted to positive values. As in the Metropolis algorithm new configurations \mathbf{x}' are chosen at random. Here the new configuration is accepted if

$$\Delta V = V(\mathbf{x}') - V(\mathbf{x}) < E_D. \quad (10)$$

In this case \mathbf{x}' is counted as a new configuration and the demon is set to $E_D \leftarrow E_D + \Delta V$, otherwise the step is rejected. Pictorially the demon might be viewed as a tiny thermometer thrown into a large swimming pool. If we denote the cluster system by A_C , the demon system by A_D and the combined system by A^0 , the conservation of energy can be written as $E_C + E_D = E^0$. The expansion of $\ln Z$ in a Taylor series yields

$$\ln Z_C(E^0 - E_D) = \ln Z_C(E^0) + \sum_i \frac{(-1)^i}{i!} \left[\frac{\partial^i \ln Z_C}{\partial E_C^i} \right]_{E^0} E_D^i. \quad (11)$$

While the first derivative is easily identified as β

$$\left[\frac{\partial \ln Z_C}{\partial E_C} \right]_{E^0} \equiv \beta \quad (12)$$

the higher derivatives are in turn derivatives of β . The probability distribution for the demon energy is now given by

$$P(E_D) = C \exp \left(-\beta E_D + \frac{1}{2} \left[\frac{\partial \beta}{\partial E} \right]_{E_0} E_D^2 \dots \right) \quad (13)$$

In the case that the demon energy is sufficiently small compared to the total energy of the system, β is indeed the inverse of the demon energy as stated in the literature [7,11].

$$\langle E_D \rangle = \int_0^{E^0 - V_0} dE_D E_D P(E_D) = \frac{1}{\beta} \quad (14)$$

C. Multiple normal modes

In the multiple normal modes (MNM) model, described in detail in [6], we take into account several isomers of a cluster, characterizing each isomer by its binding energy, permutational degeneracy, and normal modes spectrum.

The ensemble partition functions are constructed from the single isomer partition functions with proper ensemble dependent weights.

For the statistical equilibrium of isomers, the calculated one-isomer partition functions have to be multiplied by a factor σ_i reflecting the permutational degeneracy R_i . In order to relate all of them to a common energy (all particles free) also the exponential of the binding energy E_i appears as a relative weight between configurations in the canonical partition function

$$Z = \sum_i \sigma_i e^{-\beta E_i} Z_i \quad . \quad (15)$$

Within the normal modes analysis for a given isomer the potential energy is expanded up to second order around the ideal equilibrium position of the isomer.

$$V(\mathbf{x}) = \sum_{\alpha > \beta} v(r_{\alpha\beta}) \approx \frac{1}{2} \sum_{\alpha\beta ij} P_{\alpha\beta}^{ij} x_{\alpha}^i x_{\beta}^j \quad (16)$$

where x_{α}^i be the i 'th spatial component of the position of the particle α with respect to its ideal equilibrium position, $x_{\alpha}^i = 0$. Diagonalization of the matrix \mathbf{P} yields the $6N-6$ eigenfrequencies ¹.

All investigated isomers were copied from “snapshots” of MC-calculations or constructed “by hand” and relaxed numerically until the internal forces were smaller than $10^{-12}\epsilon/\sigma$. Then the matrix \mathbf{P} was calculated and diagonalized numerically. With ω_k^i being the k -th eigenfrequency of the i -th isomer, the canonical partition function is

$$Z = \sum_i \sigma_i e^{\beta E_i} \prod_{k=1}^{3N-6} \frac{2\pi}{\beta \omega_k^i} \quad . \quad (17)$$

¹Six eigenvalues vanish due to zero total momentum and total angular momentum.

(In the case of fully linear structures one has $6N-5$ eigenfrequencies.)

TABLE I. Total binding energy and relative degeneracies of the most important Ar₁₃ isomers.

Isomer	$E_{\text{bind}}/\varepsilon$	R
pure icosahedron	44.33	1
singly decorated	41.47	180
doubly dec., neighb.	40.62	900
doubly dec., dist.	39.71	4800

For the microcanonical partition function at first one has to calculate the micro-canonical MNM-partition function for one isomer from the phase space integral

$$Z_i^\mu(E) = \int (dp dq)^{3N-6} \delta(\varepsilon(q, p) - E) \quad (18)$$

$$= O_{6N-12} \frac{1}{2E} \prod_{k=1}^{3N-6} \frac{2E}{\omega_k^i} \quad (19)$$

where O_n is the surface of the n -dimensional unit-sphere. To obtain the MNM-partition function, all isomer-partition functions have to be related to a common reference-energy, and summed up with the relative permutational degeneracies σ_i ,

$$Z^\mu(E) = \sum_i \sigma_i Z_i^\mu(E - E_i). \quad (20)$$

From (17) and (20) now all thermodynamic properties can be calculated.

III. RESULTS

The multiple normal modes model gives a unique chance to study the differences between microcanonical and canonical ensembles, because for both ensembles all thermodynamic quantities can be calculated exactly. Fig.1 shows the caloric curves for Ar₁₃ clusters. In our model calculations the four most

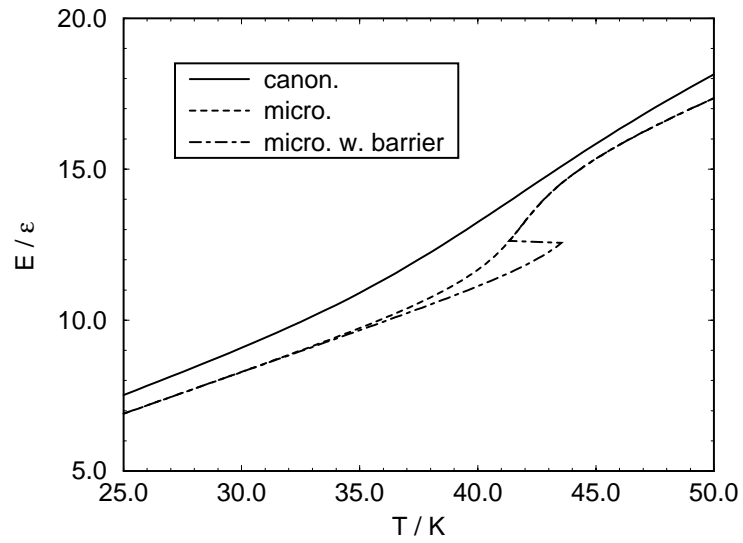


FIG. 1. Canonical versus microcanonical caloric curve of Ar_{13} calculated within the MNM model. The inclusion of a virtual activation barrier between the icosahedral and the singly decorated isomer of about 60 meV in the microcanonical model results in a van der Waals loop which is often encountered in molecular dynamics simulations.

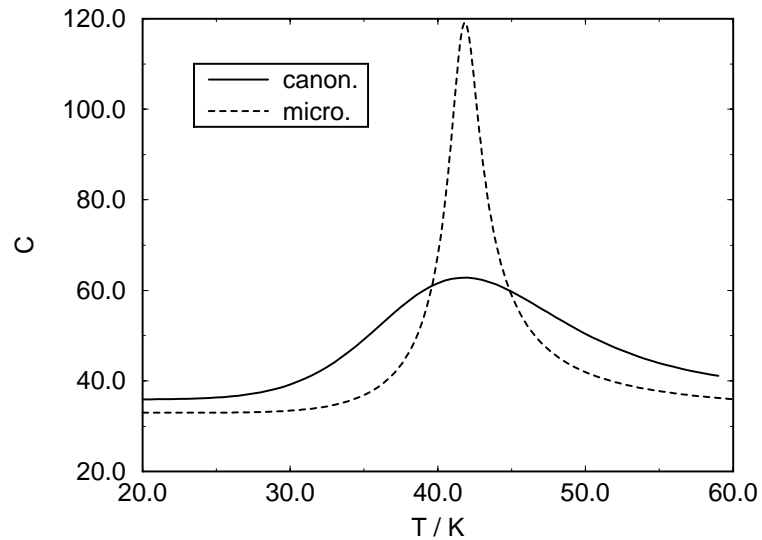


FIG. 2. Canonical versus microcanonical specific heat of Ar_{13} calculated within the multiple normal modes model.

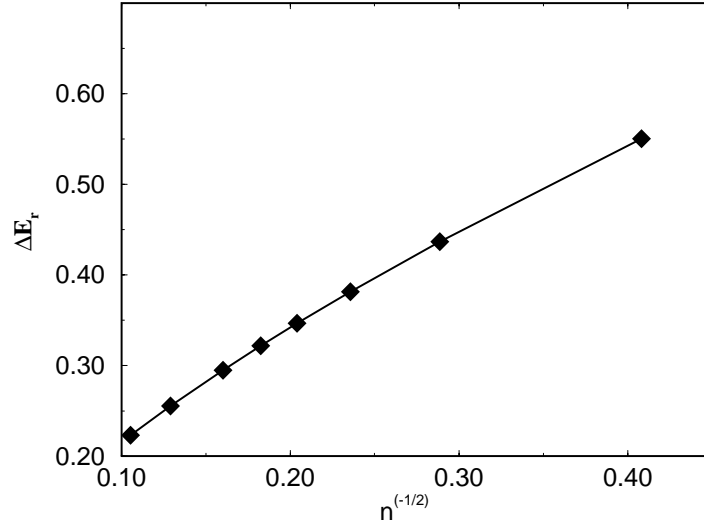


FIG. 3. Dependence of the relative energy fluctuation on the number of degrees of freedom calculated with canonical Monte Carlo at $T \approx 5$ K.

important isomers of Ar_{13} , for which the binding energies and relative degeneracies are given in Table 1, have been included. Both curves have a similar form but differ significantly by a certain amount of energy. A quite nice feature of the model is that the so-called van der Waals loops, often encountered in molecular dynamics simulations, can qualitatively be reproduced by insertion of an activation barrier into the microcanonical model, i.e. by reducing the accessible phase space up to a specified energy barrier. The differences between the ensembles get more drastical if one examines the specific heat (see Fig. 2). The phase transition occurs in both descriptions at the same temperature but is much sharper in the microcanonical ensemble.

Besides the deficiency, that within the multiple normal modes model only harmonic excitations of each isomer are considered, it is very difficult to find all important isomers and their permutational degeneracy as the cluster size increases. In Monte Carlo calculations these features are included automatically, but they are exact only within the limit of infinite computation time.

Fig.3 shows the dependence of the relative energy fluctuation (1) as a function

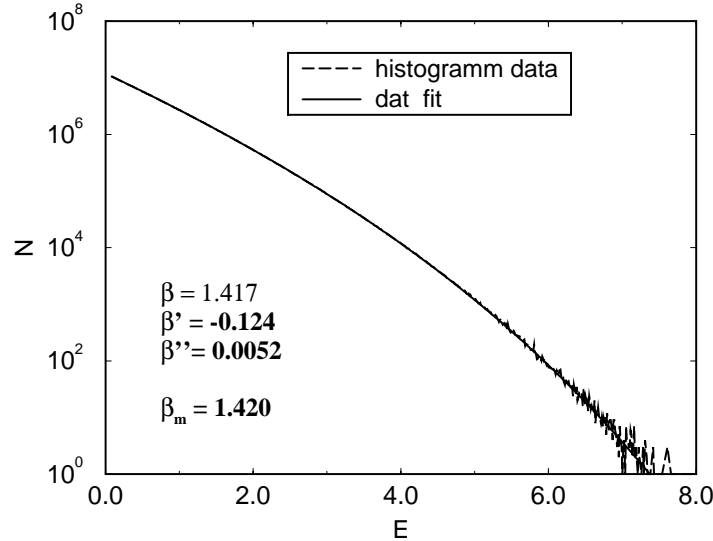


FIG. 4. Fit of the demon energy histogram data to the theoretical probability distribution function (13). The histogram was obtained for an Ar_{13} cluster at $E = -445$ meV. β_m is obtained from the mean value equation (14).

of the cluster size at a temperature of ≈ 5 K calculated from canonical Monte Carlo simulations. As expected, $1/\Delta_R E$ is approximately proportional to the inverse of the square root of the particle number.

To get comparable results between microcanonical and canonical simulations a primary task is to calculate the temperature within the microcanonical simulations. The simple choice to do that is, of course, making use of equation (14) by neglecting the higher order terms. Besides that we tried another way, which enables us to calculate the derivatives of β , too, by fitting the histogram data of the demon energy to the probability function (13). Fig. 4 displays an example of such a fit. Albeit the difference between the calculated β 's is quite small it is not negligible. By chance we have found a cheap way to calculate the derivatives of β .

The caloric curves of our Monte Carlo simulations reveal a behavior very similar to that found within the MNM model (see Fig. 5). Preliminary results show that the relative fluctuations of the temperature in the microcanonical

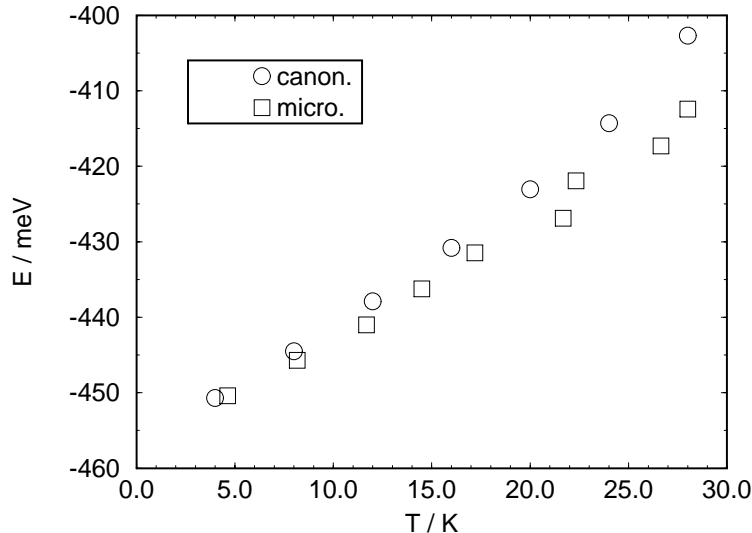


FIG. 5. Caloric curve for Ar_{13} from microcanonical and canonical Monte Carlo simulations. Every data point was evaluated with $8 * 10^7$ steps.

ensemble decreases similar to the relative energy fluctuation shown in Fig. 3 for the canonical ensemble. It is very difficult to compare the results for the higher moments of the different ensemble quantitatively because the differences depend not only on the particle number but also very strongly on the temperature (see Fig.2.). Probably other systems with a smaller transition phase, e.g. Ising systems, are more appropriate for a quantitative study of such dependencies. Nonetheless the decrease of the relative fluctuations of the state variables with increasing system size in both ensembles indicates that the differences between the ensembles decrease with $\approx N^{-1/2}$, too.

IV. CONCLUSIONS AND OUTLOOK

We have shown that in the case of small systems it is not unimportant which thermodynamical ensemble is used to describe the clusters. Things might get more interesting if more state variables are considered, e.g. by introducing spin degrees of freedom along with a coupling to an external magnetic field. A study for such a system is in preparation. To investigate the

size dependencies more properly not only the range of the cluster size (in this study up to 40) has to be expanded. Because of possible magic number effects in every size region some neighbor numbers should be considered in order to average out such effects.

The accurate calculation of higher moments, or derivatives of β within the microcanonical ensemble, remains a problem to be solved. One solution could be to invent a procedure similar to the optimized data analysis of Ferrenberg.

REFERENCES

- [1] T.L. Hill: J.Chem.Phys. 36(12), 3182 (1962).
- [2] T.L. Hill, *Thermodynamics of Small Systems*, W.A. Benjamin Pub., New York, 1963.
- [3] L.E. Reichl, *A Modern Course in Statistical Physics*, Edward Arnold, London, 1991.
- [4] H.L. Davis, J. Jellinek, R.S. Berry: J. Chem. Phys. **86**, 6456 (1987)
- [5] P. Borrmann: COMMAT **2**, 593 (1994)
- [6] G. Franke, E.R. Hilf, P. Borrmann: J. Chem. Phys. **98**, 3496 (1993)
- [7] M. Creutz: Phys. Rev. Lett. **50**, 1411 (1983)
- [8] D.J.E. Callaway, A. Rahman: Phys. Rev. Lett. **49**, 613 (1982)
- [9] M.J. Grimson: Chem. Phys. Lett. **195**, 92 (1992)
- [10] M.S.S. Challa, J.H. Hetherington: Monte Carlo Simulations using the Gaussian Ensemble, in: *D.P. Landau, K.K. Mon, H.-B. Schüttler, Springer Proceedings in Physics Vol 33: Computer Simulation Studies in Condensed Matter Physics, Springer Verlag, Berlin, 1988.*
- [11] M. Creutz, P. Mitra, K.J.M. Moriarty: J. Stat. Phys. **42**, 823, (1986)
- [12] N. Metropolis, A. Rosenbluth, M. Rosenbluth, A. Teller, E. Teller: J. Chem. Phys. **21**, 1087 (1953)
- [13] A.M. Ferrenberg, R.H. Swendsen: Phys. Rev. Lett. **63**, 1195 (1989)
- [14] A.M. Ferrenberg, R.H. Swendsen: Phys. Rev. Lett. **61**, 1195 (1988)

Kapitel 6

**How should thermodynamics
for small systems be done?**

How should thermodynamics for small systems be done ?

Peter Borrmann

Department of Physics, University of Oldenburg, D-26111 Oldenburg, Germany

Abstract

We show, that the question of which simulation method is the right one to describe the thermal behaviour of clusters, is not a philosophical one. Moreover we point out, that getting *better* results might be accompanied by a *loss* of information. Different points of view yield different results.

The number of iterations, let us call it simulation time, plays a central role here. Making use of the simulation data at higher temperatures the phase transitions and the effects of isomerisation are easy to understand.

I. INTRODUCTION

This paper is imposed to stimulate the discussion concerning thermodynamics and statistical mechanics of small systems. We will study in the case of small atomic clusters the theorem of statistical mechanics, that the long time average of observables of systems corresponds to the ensemble average. A second topic will be a detailed exhibiting of phase transitions as intruding of configuration isomer contributions.

Argon clusters are theoretically and experimentally the best investigated clusters. Early work on phase transitions of Argon clusters has been done by

Berry et.al [5–7]. They have been shown by a simple model and a classical molecular dynamics study for the case of Ar_{13} , that small Ar clusters exhibit a broad thermal transition, which is termed 'solid-liquid' like.

Phase transition like behaviour of clusters is understood as a mixing of different isomers. The transition from *solid like* to *fluid like* behaviour is known to be smooth exhibiting a so-called coexistence phase. Isomerisation effects have also recently been studied by Franke et.al. [12] for Ar_6 and Ar_{13} clusters.

In this study we concentrate on the thermal behaviour of clusters within the coexistence phase in quantum mechanical treatment.

The calculations are done by Path Integral Monte Carlo and classical Metropolis Monte-Carlo simulations.

II. COMPUTATIONAL METHOD

A. Path Integral method

In this study we consider only interatomic forces between the atoms of the Ar_N cluster, neglecting electronic excitations, fine structure splitting and so on. The Hamiltonian we apply, is given by

$$H = \sum_{i=1}^N -\frac{\hbar^2}{2m} \frac{\partial^2}{\partial \mathbf{r}^2} + \sum_{i<j}^N V(r_{ij}) \quad (1)$$

where $V(r)$ stands for the commonly used Lennard-Jones Potential

$$V(\mathbf{r}) = 4\epsilon \left(\left(\frac{\sigma}{r} \right)^{12} - \left(\frac{\sigma}{r} \right)^6 \right) \quad (2)$$

with parameters $\sigma = 3.405 \text{ \AA}$ and $\epsilon = 10.3 eV$.

The temperature behaviour of the system is calculated using the Path Integral Monte-Carlo technique. Since time scales have some importance for our considerations, we give a short description of the used special algorithm .

The basic quantity we have to calculate is the partition function Z , which - using the Feynman-Kac formula - can be written as

$$Z = \left[\int \prod_{i=1}^N \prod_{\mu=1}^M d\mathbf{r}_i(\mu) \right] \left(\frac{Mm}{2\pi\beta\hbar^2} \right)^{\frac{3M}{2}} \exp \left(- \sum_{\nu=1}^M \frac{Mm}{2\beta\hbar^2} \sum_{i=1}^N (\mathbf{r}_i(\nu) - \mathbf{r}_i(\nu+1))^2 \right) \times \quad (3)$$

$$\exp \left(- \frac{\beta}{M} \sum_{\nu=1}^M \sum_{i < k}^N V(r_{ik}(\nu)) \right) + O(\beta^3 M^{-2})$$

with the condition $\mathbf{r}_i(M+1) = \mathbf{r}_i(1)$.

The parameter M is the number of *time slices* or intersections of the quantum paths numerically taken into account. For Ar-clusters we achieved good convergence taking $M = [80/T]$.

The evaluation of 3 is performed with a Metropolis algorithm consisting of macroscopic and microscopic steps. Within a macroscopic step all microscopic coordinates $\mathbf{r}_i(\mu)$ ($\mu = 1..M$) are moved at one time. In every microscopic step all microscopic coordinates are moved successively. The macroscopic steps are used to provide a *fast* scanning of the configuration space. The case $M = 1$ corresponds to classical description of the system.

Although 3 is formally exact, our calculations are limited by computation time. The real time of a simulation can be estimated roughly by the following considerations. In the classical system the mean value of the absolute velocity is given by $v_{\text{rms}} = \sqrt{3kT/m}$. Comparing this value with the mean length Δs_{macro} and Δs_{micro} of our Metropolis steps, the simulation time is estimated by

$$t_{\text{sim}} \approx N_{\text{it}} \sqrt{\frac{m}{3kT}} (\Delta s_{\text{micro}} + \Delta s_{\text{macro}}), \quad (4)$$

where N_{it} is the number of iterations.

In all calculations we have chosen N_{it} to yield a simulation time $t_{\text{sim}} \approx 10^{-6} \text{s}$.

B. Optimized Data Analysis

Making use of the optimized Monte Carlo data analysis method of Ferrenberg and Swendsen [8,9], which is based on an earlier idea of Bennett [10], the results of our Metropolis simulations can be improved substantially. For convenience we give a short outline of the method. If we perform R Metropolis simulations at parameters β_i and store the Monte Carlo data as histograms $N_\beta(E)$ with n_{β_i} being the total number of observations in the i 'th run, the probability distribution is given by

$$P_\beta(E) = N_\beta(E)/n_\beta = W(E) \exp(-\beta E + \beta F), \quad (5)$$

where $W(E)$ is the density of states, and F is the Helmholtz free energy. Following Ferrenberg et.al. the normalized probability distribution can be improved by

$$D_\beta(E) = \frac{\sum_{i=1}^R N_i(E)}{\sum_{i=1}^R n_i \exp(-(\beta_i - \beta)E + \beta F_i)} \quad (6)$$

where

$$\sum_E D_{\beta_i} = \exp(\beta F_i), \quad (7)$$

which is simply the partition function. The values of F_i can be determined within an additive by selfconsistent iteration of 6 and 7. Simply spoken, this method improves $D_\beta(E)$ by use of simulation data at other histogram data weighted by the number of observations. We slightly improved the method by using fitted probability distributions which are sacrificed by χ^2 tests.

Now the mean value of any observable $O(E)$ can be calculated easily as a function of β .

$$\langle O_\beta(E) \rangle = \frac{1}{Z_\beta} \cdot \int_E O(E) D_\beta(E) \quad (8)$$

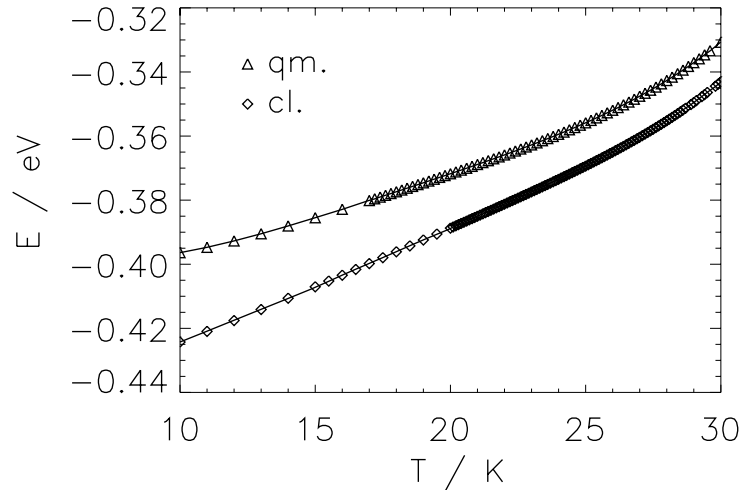


FIG. 1. Total energy versus temperature for Ar_{13} clusters. Quantum mechanically data points \triangle and classically calculated data points \diamond are connected using shape preserving cubic spline.

III. RESULTS

Fig. 1 shows the total energy and the potential energy of Ar_{13} versus temperature calculated from 3 quantum mechanically and classically. From this curve it can be seen that the quantum mechanical energy differs from classical energy at zero point by about 14 %, as has also been reported in [12]. Nonetheless, the qualitative melting behaviour is quantum mechanically and classically very similar. Fig.2 shows the specific heat of Ar_{13} clusters. The marked points are calculated directly from simulation data, the solid lines by appropriate differentiation of the smoothed caloric curve. The relative good coincidence is very satisfying, because the calculation of derivative quantities like C in PIMC is quite difficult with relative errors at about one order of magnitude larger than that of the energy. A plot of the root mean square bond length fluctuation δ versus temperature is remarkable and elucidating:

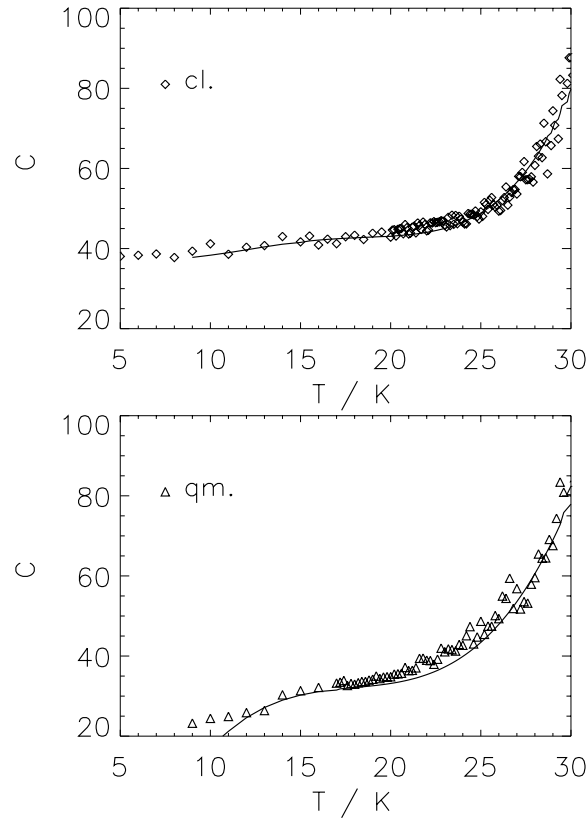


FIG. 2. Spec. heat versus temperature for Ar_{13} clusters. Quantum mechanical data points \triangle and classically calculated datapoints \diamond are connected using shape preserving cubic spline.

$$\delta = \frac{2}{n(n-1)} \sum_{i < j}^n \frac{(\langle r_{ij}^2 \rangle - \langle r_{ij} \rangle^2)^{1/2}}{\langle r_{ij} \rangle} . \quad (9)$$

The starting point of the melting phase slightly differs quantum mechanically and classically by about 2.5 K. Strong fluctuations within the melting phase occur in both cases.

On this subtle effect we will now concentrate. Looking somewhat closer at the δ -plot we see in both cases a light bifurcation in the starting region of the coexistence phase. The effect is more prominent in the q.m. case. This result is very similar to that reported by Berry [13] for Ar clusters in cavities. We interpret this discontinuity as an effect of simulation time. At higher

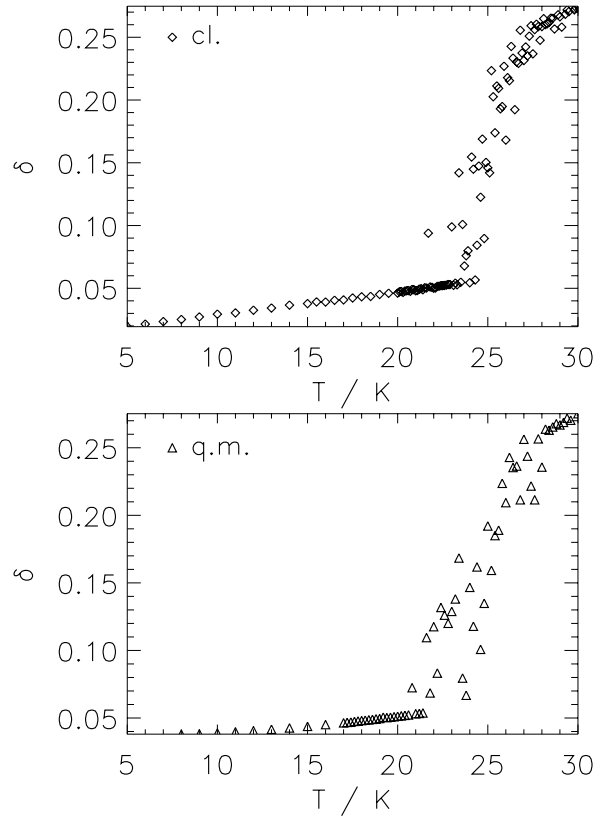


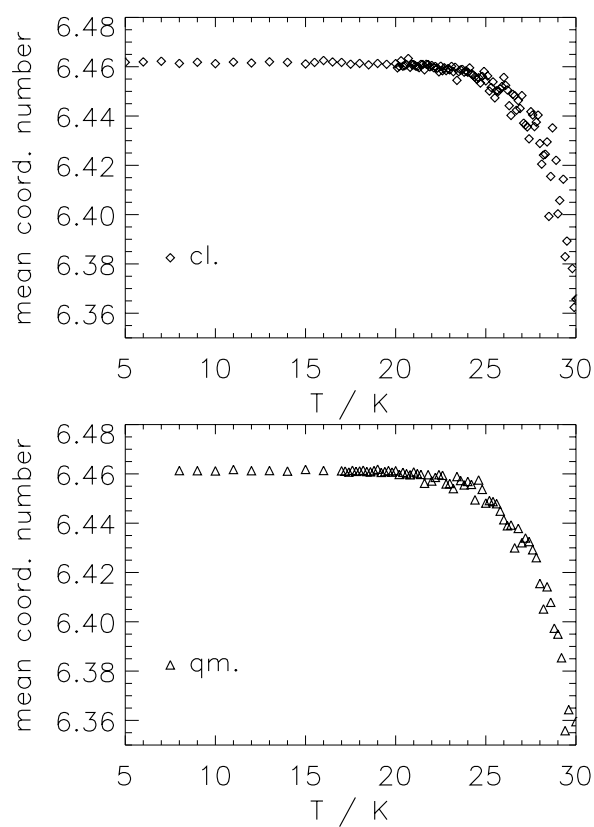
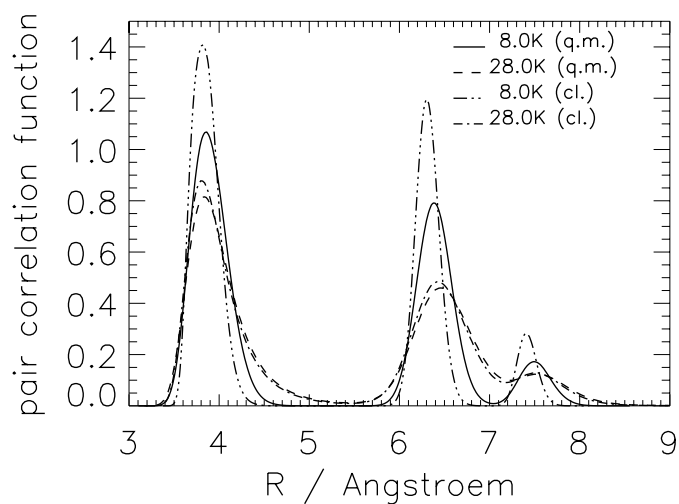
FIG. 3. Root mean square fluctuation versus temperature for Ar_{13} clusters.

temperatures the system starts to access the less stable isomers besides the icosahedron. The mobility of the argon atoms strongly depends on temperature and thus on the average time the system needs for a transition from one isomer state to another. A similar bifurcative behaviour can be seen in the plot of the mean coordination number, i.e. the average number of nearest neighbours, which is 6.642 for the pure icosahedron and 6.00 for the second stablest isomer, the singly decorated icosahedron (one atom moved into the next shell). Note, that even at 30 K the system is in the icosahedron state most of the time.

A comparison of the q.m. and cl. pair correlation functions (Fig.4 and Fig.5)

$$\Gamma(r) = \left\langle \frac{2}{N(N-1)} \sum_{i<j}^N \delta(|\mathbf{x}_i - \mathbf{x}_j| - r) \right\rangle, \quad (10)$$

which serves as another indicator for structural transformations shows, that

FIG. 4. Mean coordination number for Ar_{13} clusters.FIG. 5. Pair correlation function of Ar_{13} clusters for various temperatures.

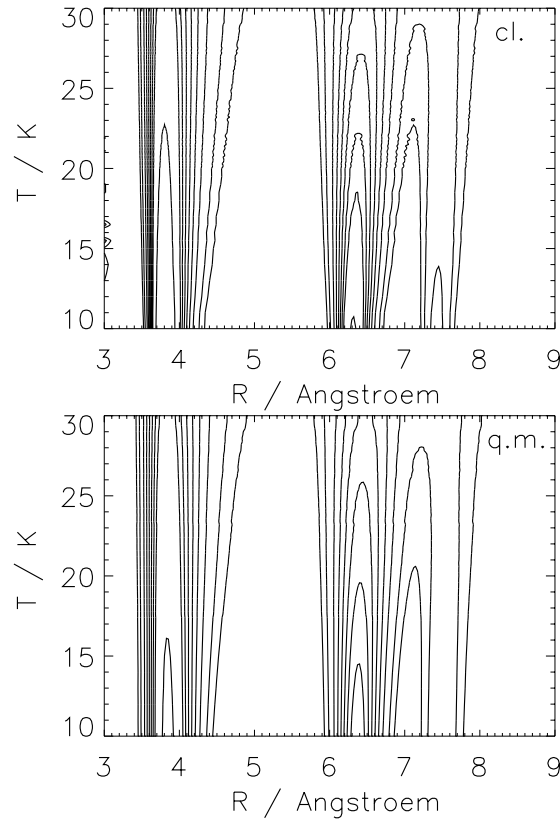


FIG. 6. Contour plots of the pair correlation for Ar_{13} clusters.

the distributions are quantum mechanically broader for low temperatures, but the difference gets smaller with increasing temperature and is almost vanished in the coexistence region. [*]

For Ar_6 clusters we have two important isomers, the tritetrahedron and the octahedron. Here we see from the pair correlation function (Fig.7) as well as from the root mean square bond length fluctuation, that the tritetrahedron, which is indicated through the third hump in the pair correlation function, can be accessed only above 8 K. We have plotted δ versus T for two different iteration times, $2 * 10^6$ and 10^8 iterations. As expected, the curve for the larger iteration time is much smoother, but if there is bifurcation for the short computer runs, it is not as well identifiable as for Ar_{13} . The plot of the

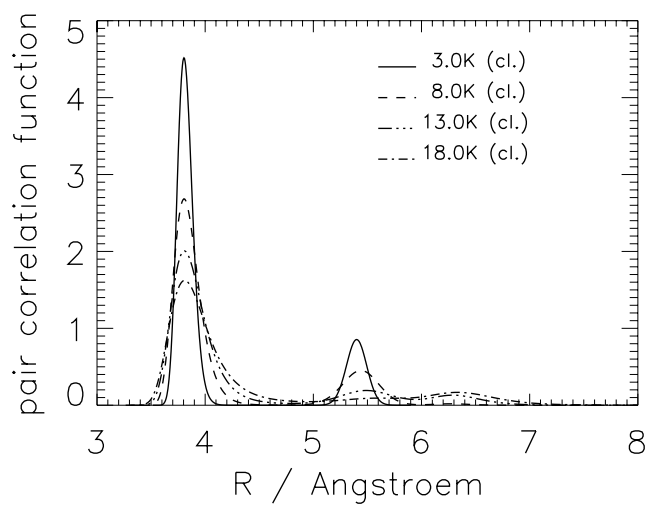


FIG. 7. Pair correlation function from classical simulation of Ar₆ clusters.

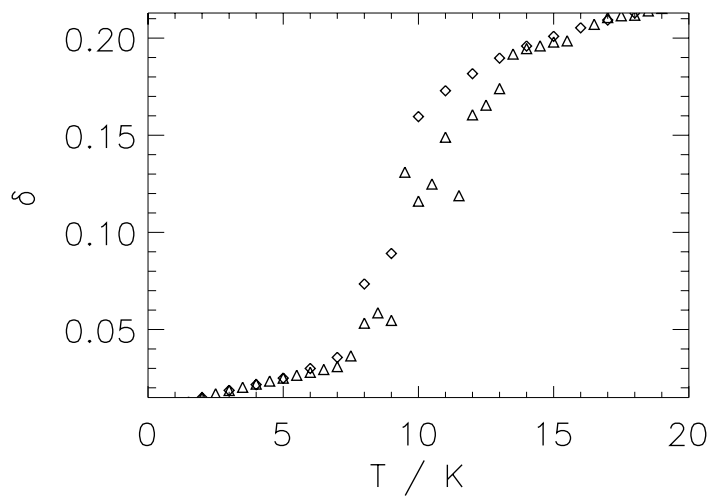


FIG. 8. Root mean square fluctuation versus temperature for Ar₆ clusters. The diamonds \diamond are calculated classically using 10^8 iterations, the triangles \triangle , using 2×10^6 iterations.

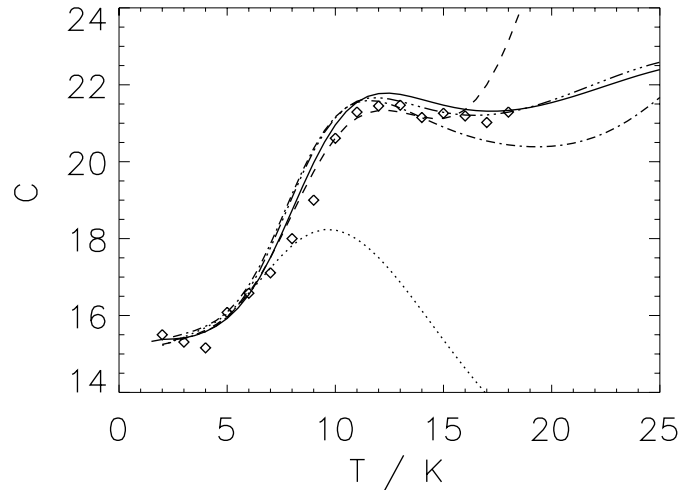


FIG. 9. Specific heat of Ar_6 clusters. The diamonds \diamond indicate the specific heat calculated from simulations with 10^8 iterations each. The solid line is calculated with the histogram method using the histograms of all simulations. The dotted line is calculated from the histogram at 4.0 K, the dashed line from 10.0 K, the dashed-dotted line from 14.0 K and the dashed-triple dotted line from 18.0 K.

specific heat C is now the most interesting one. We used the Ferrenberg method to recalculate C from our simulation data. Using only the data from this computer experiment at 14.0 K we get an almost perfect fit over the whole temperature range. An interesting point is that even for the solid line, which is perfect in the sense that information from all runs is used, the specific heat drops slightly after melting.

Nonetheless, much more interesting is the plot using only the data from the 4.0 K run. As in the case of solids the specific heat drops drastically after the transition point. The effect results clearly from the fact, that at 4.0 K the system does not *know* about the second isomer. Clearly this curve would be the right one, if we viewed our system as a dilute gas of Ar-octahedrons, but not if we say our system is a dilute gas of Ar_6 clusters.

Indeed we think to get a maximum of information by using the optimized

data method with different combination of simulation data. We hope that our last figure makes clear the deficiencies of pure Molecular Dynamics and Monte Carlo methods. In the case of Molecular Dynamics energy conservation sometimes strictly forbids transition from one isomer to another. This is in principle possible in Monte Carlo, but often takes place very slowly. One solution would be to start simultaneous runs with different isomer start configurations together with appropriate recalculation taking into account the degeneracies of the isomers and so on.

Beside the fact, that it would be difficult to detect in which isomer state the system is, this method gets completely unpracticable with growing particle and *exploding isomer* number within simulations.

A principal question has been left open so far. If the iteration time is sufficiently large, single Ar atoms evaporate from the cluster even at low temperatures. This fact clearly collides with the demand of the correspondence theorem of a long time average. If we are dealing with thermodynamic equilibria or are not, has to be decided very carefully from case to case.

IV. CONCLUSIONS AND FUTURE INVESTIGATIONS

Especially the higher moments of thermodynamic equations are expected to be of further interest. As pointed out by T.L. Hill [1,2], fluctuation quantities become more significant for smaller systems, whereas they are in general unimportant for macroscopic systems.

The quantum mechanical treatment and larger cluster sizes are worth being pursued further. Because we have to deal with *short time equilibria* quantum mechanical *tunneling* from one isomer to another may yield really strange effects at first look. Suppose for example that a second isomer gets accessible

very suddenly. This would increase the density of states resulting in a drop of energy and entropy with increasing temperature and thus in a breaking of thermodynamic laws.

ACKNOWLEDGMENTS

Part of the computations have been done on the Siemens S400 of *Regionales Rechenzentrum Niedersachsen* RRZN in Hannover.

REFERENCES

- [1] T.L. Hill, J.Chem.Phys. 36(12), 3182 (1962).
- [2] T.L. Hill, *Thermodynamics of Small Systems*, W.A. Benjamin Pub., New York, 1963.
- [3] R.P. Feynman, A.R. Hibbs, *Quantum Mechanics and Path Integrals*, McGraw-Hill, New York, 1965.
- [4] N. Metropolis, A. Rosenbluth, M.N. Rosenbluth, A.H. Teller, E. Teller, J.Chem.Phys. **21**, 1087 (1953).
- [5] S. Berry, J. Jellinek, G. Natanson, Chem.Phys.Lett. **107**(3), 227 (1984).
- [6] J. Jellinek, T.L. Beck, S. Berry, J.Chem.Phys **84**(5), 2783 (1986).
- [7] S. Berry, J. Jellinek, G. Natanson, Phys.Rev.**A** **30**(2), 919 (1984).
- [8] A.M. Ferrenberg, R.H. Swendsen, Phys. Rev. Lett. **63**, 1195 (1989)
- [9] A.M. Ferrenberg, R.H. Swendsen, Phys. Rev. Lett. **61**, 1195 (1988)
- [10] C.H. Bennett, J. Comp. Phys. **22**, 245 (1976)
- [11] M.F. Trotter, Proc.Am.Math.Soc. **10**, 545 (1959).
- [12] G. Franke, E.R. Hilf, P. Borrmann, J.Chem.Phys **98**(4), 3496 (1993).
- [13] Feng Yin Li, R.S. Berry, Z.Phys. **26**, 394 (1993)

* In a forthcoming study we will show, that this is not the case for Ne clusters, because there quantum effects are much stronger. For example the ground state energy is nearly 40 % of the binding energy.

Kapitel 7

Magnetism of small transition metal clusters and the effects of isomerisation

Magnetism of small transition metal clusters and the effects of isomerisation

Peter Borrmann, Bernd Diekmann, Eberhard R. Hilf

Department of Physics, Carl v. Ossietzky University Oldenburg, D-26111

Oldenburg, Germany

David Tománek

Department of Physics and Astronomy, and Center for Fundamental Materials

Research, Michigan State University, East Lansing, Michigan 48824-1116, USA

Abstract

We investigate the magnetic properties of small transition metal clusters using a simple statistical model which requires some input data from *ab initio* spin-density functional calculations. In our study, we consider a thermodynamically equilibrated ensemble of clusters with different structures, spin multiplicities, and ground state energies. We calculate the physical properties of this system by weighting the individual configurations according to the Boltzmann statistics. We find that presence of isomers with very similar ground state energies, yet very different magnetic properties, gives rise to a rich magnetic behaviour of the system which differs significantly from what would be expected for single configurations. We apply the present model to determine the magnetic susceptibility of a cluster ensemble of Langevin paramagnets. Our results show that some of the anomalies in the magnetic behaviour of transition metal clusters might be understood in the framework of our model which is, of course, limited by the extremely high

computational effort needed to obtain the input data.

I. INTRODUCTION

The magnetic properties of small transition metal clusters have been of growing interest in the past few years. However, there has not been any study about the dependence on temperature so far.

As shown in a large variety of papers (e.g. Refs. [1,2]) small clusters exhibit, unlike the bulk, smooth structural transformations, which one might call *isomer hopping*, and which occur between pure solid and fluid phases over a relatively wide temperature range, in a so-called coexistence phase. In the following we will be concerned with the effect of those properties on the magnetic behaviour of clusters. The basic idea is that a cluster of a specific size might have two or more structures with different magnetic moments and that these structures or *isomer states* occur with their statistical probability.¹ As shown below, this simple assumption causes a strong deviation of the paramagnetic behaviour of the magnetic susceptibility from the Curie law. As an interesting feature, a dependence on the strength of an external magnetic field might occur, even at relatively small fields. Transition metal clusters seem to be natural candidates for the occurrence of such effects because of their different possible electron configurations with very similar energies, which in turn yield quite different average magnetic moments.

¹In the following we will view different configurations as different isomers, even if they have the same symmetry and only different lattice constants.

II. THEORY

We consider to have n isomers with magnetic moments μ_i and ground state energies $E_0(i)$, calculated using an appropriate spin-density functional Hamiltonian. In the presence of an external magnetic field the energy changes. First order quantum mechanical perturbation theory yields

$$H_m = g\mu_B M B_{\text{ext}} + \frac{e^2}{8m_e} B_{\text{ext}}^2 \sum_{\nu} \langle x_{\nu}^2 + y_{\nu}^2 \rangle, \quad (1)$$

where g is the Landé factor and the magnetic field is pointing in the z -direction (see Refs. [3,4]). The first term describes a paramagnet, which will be considered exclusively in what follows and can be described with a purely classical description [5], as

$$E_m = -\vec{\mu} \cdot \vec{H}. \quad (2)$$

Now we are able to write down the partition function as

$$\begin{aligned} Z &= \sum_i^n \int_{-1}^1 d \cos \theta \exp(-\beta E_0(i) + \beta \mu_i H \cos(\theta)) \\ &= \sum_i^n \exp(-\beta E_0(i)) \frac{2}{\beta \mu_i H} \sinh(\beta \mu_i H). \end{aligned} \quad (3)$$

Indeed this is an extremely simple partition function, which can be improved to any complexity by adding all degrees of freedom of the clusters, e.g. by substituting the summation over the isomers by integration over the whole configuration space over the atomic positions or by adding a summation over different spin multiplicities of the clusters. From Eq. (3) the average magnetic moment $\langle \mu \rangle$ and the magnetic susceptibility χ can be calculated from Eq. (3) easily [5], using

$$\begin{aligned} \langle \mu \rangle &= \frac{1}{\beta} \frac{\partial}{\partial H} \ln Z \\ &= \frac{\sum_i \exp(-\beta E_0(i)) \cosh(\beta \mu_i H)}{\sum_i \mu_i^{-1} \exp(-\beta E_0(i)) \sinh(\beta \mu_i H)} - \frac{1}{\beta H}, \end{aligned} \quad (4)$$

$$\chi = \lim_{H \rightarrow 0} \frac{\langle \mu \rangle N_m}{V H}, \quad (5)$$

if N_m/V is taken as the number of particles per unit volume.² In the case of small magnetic fields $\mu H \ll k_B T$ we get

$$\langle \mu \rangle \approx Z_0^{-1}(\beta) \sum_i^n \exp(-\beta E_0(i)) \frac{1}{3} \beta \mu_i^2 H \quad (6)$$

and

$$\chi \approx \frac{N_m}{V} Z_0^{-1}(\beta) \sum_i^n \exp(-\beta E_0(i)) \frac{1}{3} \beta \mu_i^2. \quad (7)$$

Here, $Z_0(\beta)$ is the partition function defined in Eq. (3) for zero magnetic field. Eq. (7) reveals simply that χ is a linear superposition of the susceptibilities of the individual isomers weighted by their thermal probability.

III. RESULTS AND DISCUSSION

The general behaviour of the paramagnetic susceptibility according to Eq. (7) is plotted in Fig. 1 for a hypothetical system with only two major isomer states with magnetic moments μ_1 and μ_2 and their energy difference $\Delta E = E_0(2) - E_0(1)$. Unlike a purely paramagnetic behaviour according to the Curie law, the plots reveal local minima and maxima. A similar behaviour has recently been experimentally found by Cowen *et al.* [6] for Fe₂₈ clusters in supercages of NaY Zeolite. The locations of the extrema only depend on the ratio between the magnetic moments μ_1/μ_2 and ΔE . For a given ratio μ_1/μ_2 , the position of the minimum depends in an almost linear fashion on ΔE , as can be seen in Fig. 2. The extraordinary sensitivity of these results on ΔE

²The thermal property related to χ by the dissipation-fluctuation theorem is $\gamma = -\frac{1}{\beta^2} \partial_{HH} \ln Z = \partial_H \langle \mu \rangle$.

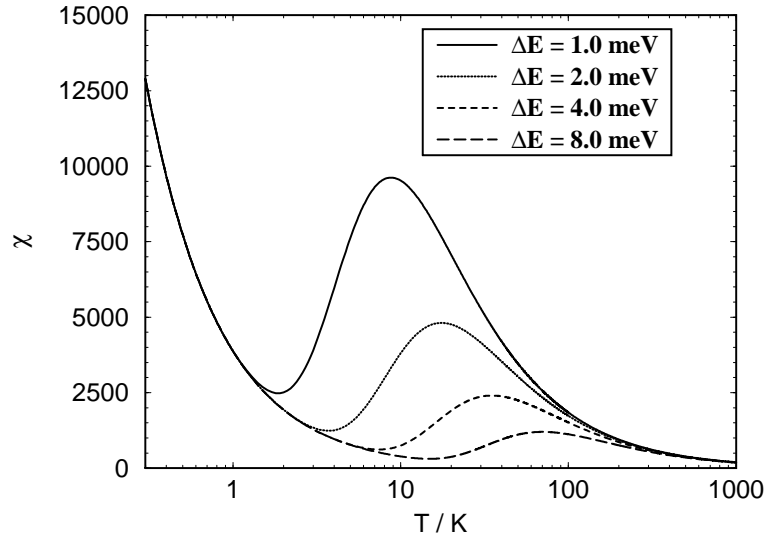


FIG. 1. Magnetic susceptibility $\chi / \mu_B \frac{N\mu}{V}$ for an ensemble consisting of two magnetic *configuration* states ($\mu_1 = 1.0 \mu_B$, $\mu_2 = 10.0 \mu_B$). ΔE is the energy difference between the two states.

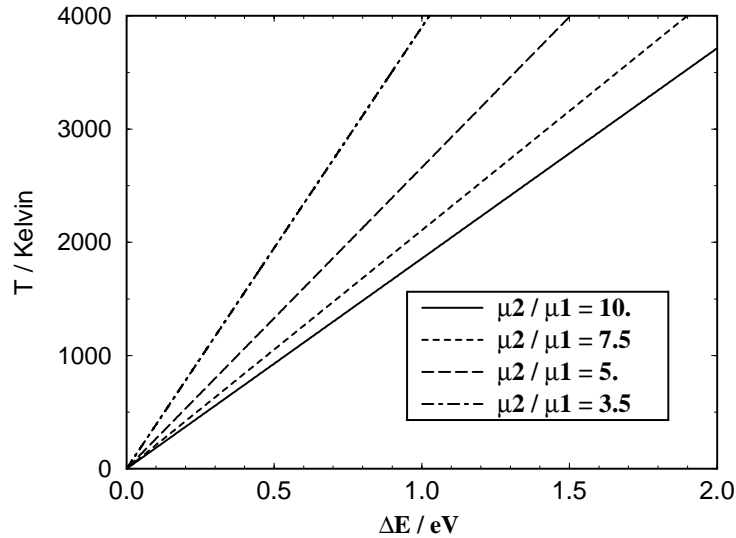


FIG. 2. Location of the local minima of the magnetic susceptibility as a function of ΔE for various ratios μ_1/μ_2 of the magnetic moments.

is illustrated by the fact that a change of ΔE by only a few meV moves the minimum by hundreds of degrees Kelvin.

In Fig. 3 the average magnetic moments of the canonical ensemble are

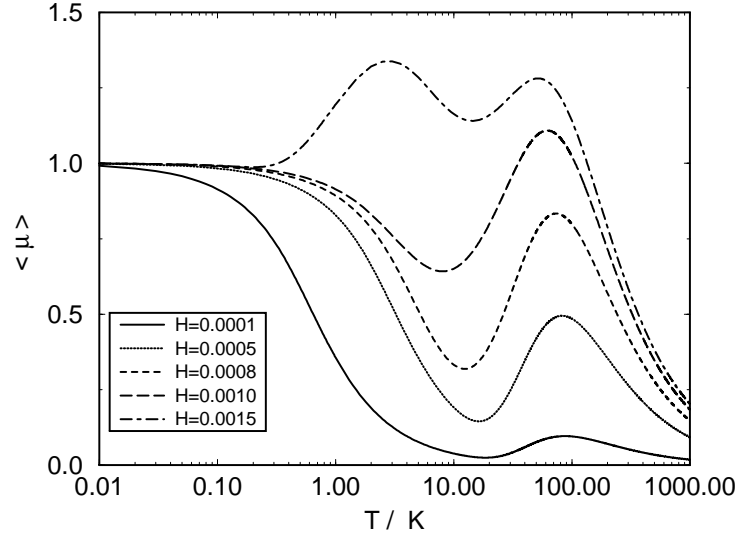


FIG. 3. Average magnetic moments at various magnetic fields H , for $\Delta E = 0.01$ eV, $\mu_1 = 1.0 \mu_B$, and $\mu_2 = 10.0 \mu_B$.

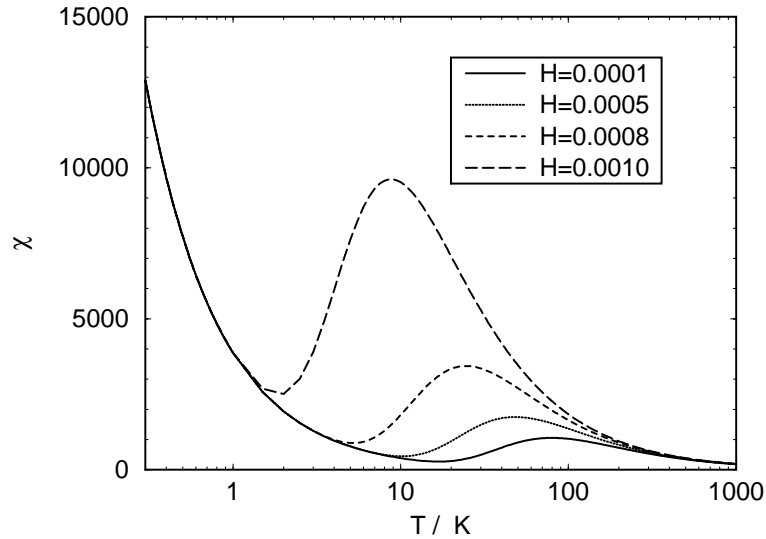


FIG. 4. Magnetic susceptibility $\chi / \mu_B \frac{N_m}{V}$ at non-zero magnetic fields H (eV/ μ_B), for $\Delta E = 0.01$ eV, $\mu_1 = 1.0 \mu_B$ and $\mu_2 = 10.0 \mu_B$.

plotted for various magnetic fields. These plots reveal the fact, that in the presence of a magnetic field the occupation probability of the isomers changes dramatically due to the additional magnetic energy.

If one views H to be small in the sense of Eq. (5), the magnetic susceptibility

TABLE I. Average magnetic moments μ (μ_B /atom) and total energy per atom E_{total} (Ry) for Cr_9 and V_9 clusters, as listed in Ref. [7].

Cr_9			V_9		
a/a.u.	μ	E_{total}	a/a.u.	μ	E_{total}
3.82	0.00	-2082.556	4.57	0.33	-1882.202
4.10	0.00	-2082.598	5.14	0.33	-1882.219
4.36	0.67	-2082.779	5.54	0.33	-1882.218
4.63	0.67	-2082.724	5.71	0.33	-1882.213
4.90	0.67	-2082.666	6.28	0.33	-1882.175
5.30	0.67	-2082.651	6.85	2.78	-1882.175
5.45	3.78	-2083.011			
6.00	3.78	-2082.934			

can be easily calculated. For varying magnetic fields this calculation yields a behavior which is very similar to that of a varying ground state energy difference (see Fig. 4).

At first sight, configurations of different symmetry – such as bcc versus fcc structures – of Fe clusters seem to be the best candidates to show the effects discussed above. Even if the energy difference between two isomers might be very small, the transition from one isomer to the other may involve a complex concerted motion of atoms and may be associated with a nonzero activation energy. Thus a thermal relaxation might take quite a long time, and a hysteresis might be observable.

Lee and Callaway [7] have found interesting results for Cr_9 and V_9 bcc clusters, which are given in Table I. With varying lattice spacing the average magnetic moment changes by a factor of up to five, whereas the ground state energy changes are only ≈ 0.04 Ry/atom. This is especially interesting since even a simple spatial expansion of the transition metal clusters intuitively is

more probable than a structural transformation.

From our results we infer that it is extremely hard to obtain phenomenological results for the magnetic behaviour of clusters from spin-density functional methods, since the results depend very sensitively on ground state energy differences, which are often very small and comparable in magnitude to the precision of these *ab initio* methods. In addition, for larger clusters, the number of relevant isomers increases dramatically.

Nevertheless, we have shown that in the model case of two cluster isomers, the rich behaviour of the magnetic susceptibility as a function of temperature and the external magnetic field is a sensitive tool to probe structural properties of clusters. On the other hand, once the general magnetic response due to the above discussed effects is understood, one might use the susceptibility of the clusters as a very sensitive thermometer.

Moreover, by applying a sufficiently strong magnetic field, one might be able to suppress one of the transition metal cluster isomers, provided the clusters have ample time for structural rearrangement. An extended study of these effects, including specific examples, will be published elsewhere.

ACKNOWLEDGEMENTS

We thank Professors J.A. Cowen and J.L. Dye for making their experimental data available to us prior to publication. One of us (DT) acknowledges financial support by the National Science Foundation under Grant Number PHY-92-24745 and the Office of Naval Research under Grant Number N00014-90-J-1396.

REFERENCES

- [1] P. Borrmann, *COMMAT* **2**, 593 (1994).
- [2] G. Franke, E.R. Hilf, P. Borrmann, *J. Chem. Phys.* **98**, 3496 (1993), cond-mat/0 10323.
- [3] M. Weissbluth: *Atoms and Molecules*, (Academic Press, San Diego, 1978).
- [4] K. Kopitzki: *Einführung in die Festkörperphysik*, (Teubner, Stuttgart, 1989).
- [5] W. Ludwig: *Festkörperphysik*, (Akademische Verlagsgesellschaft, Wiesbaden, 1978).
- [6] J.A. Cowen, K.L. Tsai, and J.L. Dye, accepted by *J. Appl. Phys.* (1994).
- [7] Keeyung Lee, J. Callaway, *Phys. Rev.* **B 48**, 15358 (1993).

Kapitel 8

Structure and Stability of polarized Li^3He_N^+ cluster ions

Structure and stability of polarized $\text{Li } ^3\text{He}_N^+$ cluster ions

P. Borrmann

Universität Bremen, Fachbereich Physik, D-2800 Bremen, Germany

E.R. Hilf

Universität Oldenburg, Fachbereich Physik, D-2900 Oldenburg, Germany

Abstract

Using the Path Integral Monte Carlo method we calculate the structural and energetic properties of small spin polarized $\text{Li } ^3\text{He}_N^+$ ($1 \leq N \leq 7$) clusters. To investigate the Pauli principle effects we perform calculations using Fermi Dirac statistics as well as Boltzmann statistics. It turns out that FD statistics affects mainly the structure of the very small clusters. Energetic effects are significant but very small. We found a dominant magic number at $N=6$. For the spatial pair correlations we find an interesting counterplay of FD statistics induced spatial hindrance due to shell occupation and the known short range 'repulsion'.

I. INTRODUCTION

Rare gas clusters have been investigated extensively in the past [1-7]. However, the effects of quantum statistics have mostly been neglected.

For ^4He clusters a number of investigations using different theoretical methods [2-4,8] have been made. Here we have chosen the interesting case of spin

polarized ^3He , known to show Pauli principle effects most strongly in the fluid phase. Their small mass and thus their high mobility result in considerable overlap of their wave functions. ^3He -clusters are most weakly bound and do not exist for $N < 5$ [9]. To allow for experimental tests of the predictions of the calculations and to bind the clusters at all we added a single Li^+ ion in the center, thus treating spin polarized $\text{Li}^+ ^3\text{He}_N$ clusters.

Here we use the Path Integral Monte Carlo method (PIMC), which is originally due to R.P. Feynman [10], as an alternative formulation of Quantum Mechanics to the Schrödinger picture. A quantum mechanical motion is calculated by summing the classical action over all classical paths, including those which temporarily break the classical conservation laws. Recently PIMC calculations have been undertaken for argon clusters by Franke, Polley and Hilf [1] and Schulte [6]. PIMC including Fermi Dirac statistics, which is a more elaborate but in this case a necessary instrument, will be applied here.

II. THE HAMILTONIAN

Within our simulations we assumed the Li^+ ion to be fixed in coordinate space. Both, the interaction between the polarized ^3He atoms and between the Li^+ and the ^3He atoms are modelled by Lennard-Jones potentials of the form

$$V(r) = 4\epsilon \left(\left(\frac{\sigma}{r} \right)^{12} - \left(\frac{\sigma}{r} \right)^6 \right).$$

Potential parameters are taken from Senff and Burton [11] to be $\epsilon_{\text{LiHe}} = 80.42$ meV, $\sigma_{\text{LiHe}} = 1.69$ Å for the Li^+ - ^3He interaction and $\epsilon_{\text{HeHe}} = 0.88$ meV, $\sigma_{\text{HeHe}} = 2.56$ Å for the ^3He - ^3He interaction.

III. METHOD

The basic quantity to be calculated is the quantum mechanical partition function

$$Z = \text{Tr} \langle \psi | \exp(-\beta H) | \psi \rangle. \quad (1)$$

For polarized fermions $|\psi\rangle$ has to be completely antisymmetric. Evaluation of (1) is performed using the Path Integral Monte Carlo (PIMC) method. In the past fifteen years PIMC has been investigated more extensively and a large number of slightly different algorithms have been proposed (see e.g. [12-20]). All algorithms are merely based on approximation of (1) through Trotter's formula [21]

$$Z = \text{Tr} \left(\exp\left(-\frac{\beta}{M}H_0\right) \exp\left(-\frac{\beta}{M}H_1\right) \right)^M + O(\beta^3/M^2).$$

H_0 and H_1 are the kinetic and the potential energy operator. The resulting $3NM$ dimensional integral is evaluated using the algorithm of Metropolis, Rosenbluth et. al. [22]. We adopted the so called primitive algorithm of Takahashi and Imada [12,13], which turned out to be favourable for the problem under consideration. Other methods are more effective on scalar computing machines but not as easily vectorizable as the above. Denoting the particle mass by m , total energy E , kinetic energy E_k , potential energy E_p , and pair correlation function $\rho(r)$ are given as follows :

$$\begin{aligned} E &= -\frac{1}{Z} \frac{\partial Z}{\partial \beta} \quad , \\ E_k &= -\beta^{-1} \frac{m}{Z} \frac{\partial Z}{\partial m} \quad , \\ E_p &= E - E_k \quad , \\ \rho(r) &= \left\langle \frac{2}{N(N-1)} \sum_{i < j}^N \delta(|\mathbf{x}_i - \mathbf{x}_j| - r) \right\rangle \quad . \end{aligned}$$

In the pictures below we normalized the highest peaks in the pair correlation functions to 1 We justified our new computer code using the harmonic oscillator

as a test system. For both statistics, particle numbers up to 15, and various temperatures analytic results for kinetic and potential energy were reproduced with an error below 0.65% .

IV. RESULTS

PIMC can be applied only for finite temperatures. For all calculations we choose a temperature of 6 K ($\cong 0.52$ meV), which is very low compared to binding energies. Thus results can be assumed to be a fair approximation for ground state properties. The quantity $\Delta^2 E$, which is commonly used to

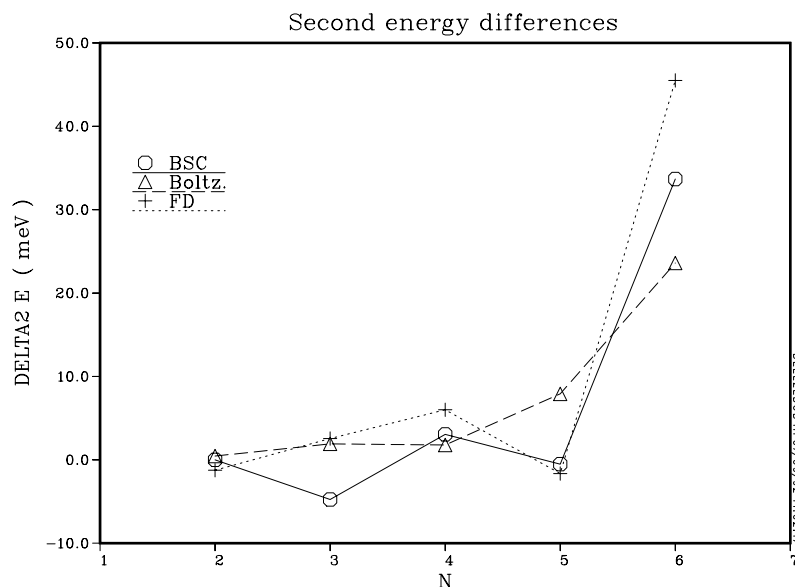


FIG. 1. Second energy differences $\Delta^2 E = E_{N+1} + E_{N-1} - 2E_N$.

indicate magic numbers of atomic clusters, is given for Fermi Dirac and Boltzmann statistics Path Integral Monte Carlo calculations and Best Single Clusters configurations in Fig.1. The latter have been obtained by minimization of the total classical potential energy (Larger values of $\Delta^2 E$ indicate more stable clusters.). The first closed shell - accompanied by a magic number - occurs at $N=6$. The corresponding geometric structure is a bipyramid with the Li^+ ion in the center. A much less intensive peak occurs at $N=4$. Binding energy per

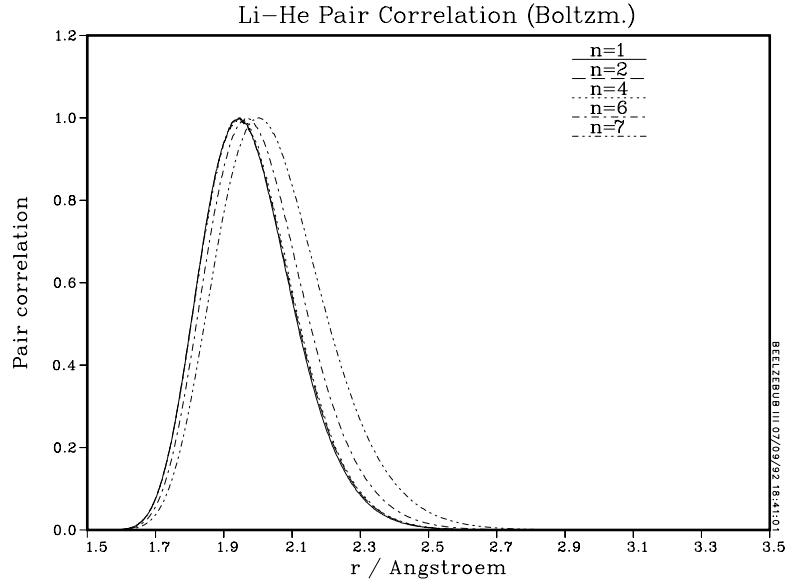


FIG. 2. Li-He pair correlation function calculated using Boltzmann statistics for various cluster sizes.

atom for cluster sizes $N > 6$ then drops rapidly. The reason for this is simply that atoms being in the second 'geometric shell' are much more weakly bound by the central Li^+ ion. The occurrence of the new geometric shell can be seen most easily by the gap between Li - He pair correlation functions for $N=6$ and $N=7$ in Fig. 2. The energy differences between the calculations for the correct quantum FD statistics in comparison to neglecting it (assuming the particles to be distinguishable) turn out to be generally small. Significant differences are seen at $N=7$, which is assumed to be due to the much more loose binding of the second shell, starting to be filled. The main interest of our investigations is the influence of Fermi statistics. The pair correlation functions for the $\text{Li}^+ \text{}^3\text{He}_2$ cluster (Fig.3) show that FD statistics lead to an additional short range repulsion between the He atoms, increasing the mean distance between them as to be expected. The true (FD statistical) calculation shows just one peak with a distribution smaller than that in the respective Boltzmann case, thus the He atoms ship more precisely into the antipode configuration. To clarify the situation we made a corresponding calculation where we turned off

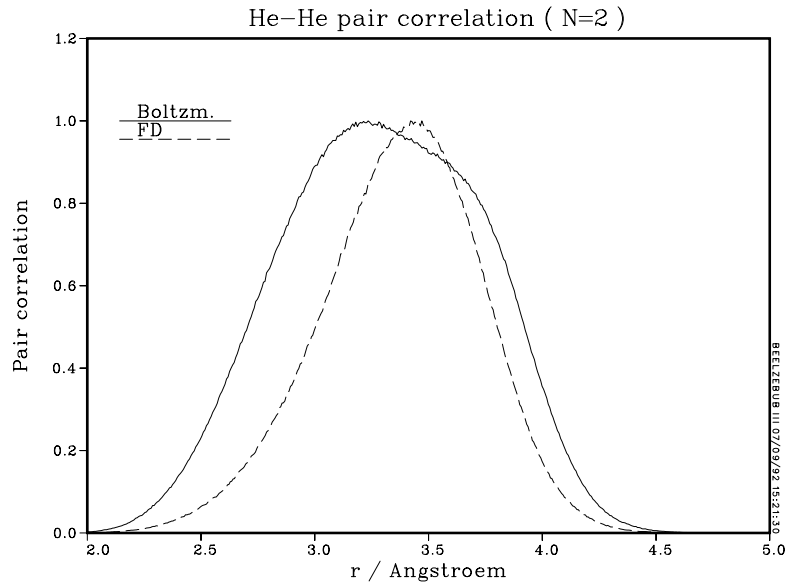


FIG. 3. He-He pair correlation function for $Li^+ He_2$.

the He-He interaction. Here the 'FD repulsion' occurs much more drastically (Fig.4). The balance of 'stay apart' and 'pick the best bound shell' can be tried as a guideline to interpret the results for the other cases. [htb] In Fig. 4

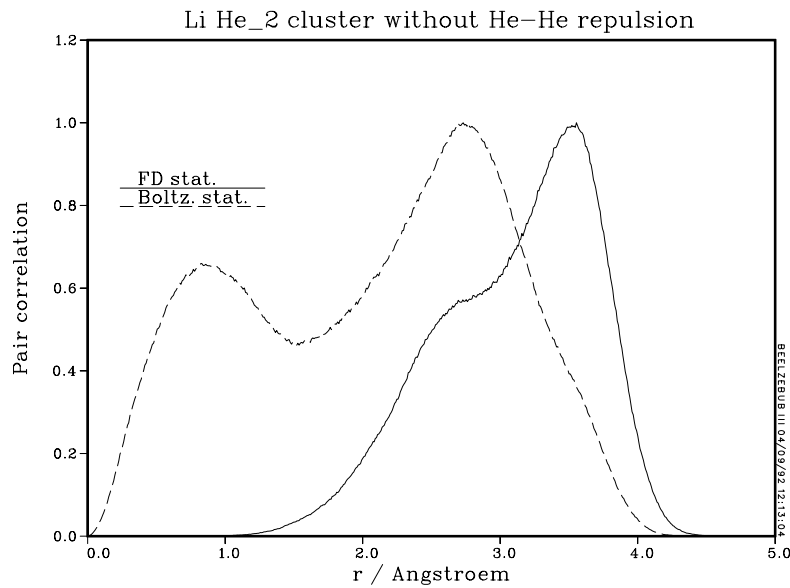


FIG. 4. He-He pair correlation calculated without He-He interaction.

and in the Boltzmann case of Fig. 3 structures interpretable as superposition of two humps can be seen. These are simply due to the spherical symmetric

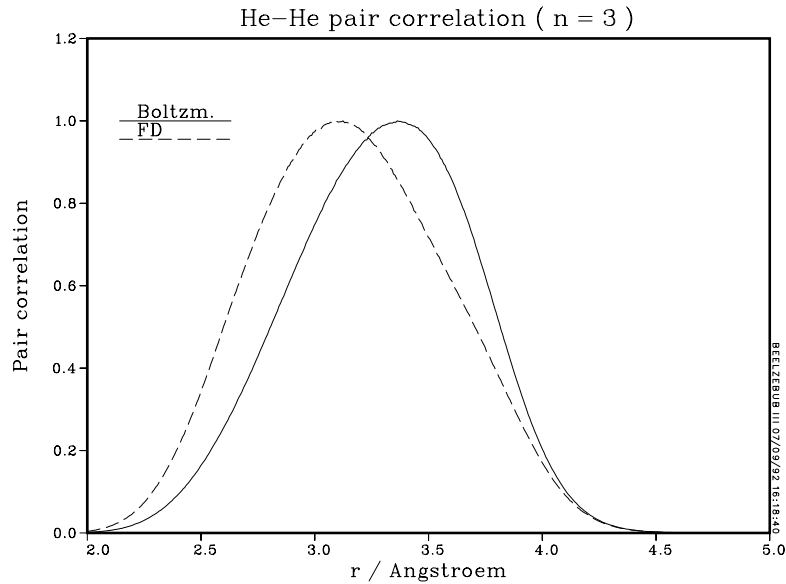


FIG. 5. He-He pair correlation function for $\text{Li}^+ \text{He}_3$.

distribution of He atoms around the central Li^+ ion. At first sight strange things occur for $N = 3$. The mean distance decreases for FD statistics (Fig.5). The only reason for this is that all He atoms tend to have maximal distances on the sphere of minimal potential. Simply spoken, if the distance between two atoms increases, another distance must decrease. For $4 \leq N \leq 6$ structural differences between statistics almost vanish, i.e. the structure seems to be completely governed by potential and geometric requirements. At $N=7$ the He atom in the outer shell is much more loosely bound. As in the case of $N=2$ the influence of the Pauli principle results in an increase of the mean distance between He atoms (see Fig.6). In our simulations for larger cluster sizes we did not achieve numerical convergence because of evaporation of one or more He atoms. Inspection of higher moments of correlation functions, e.g. the width of distribution, indicates significant influence of FD statistics on structure, too. This should be of main importance for the discussion of the 'phase' of $\text{Li}^+ \text{He}_N^+$ clusters.

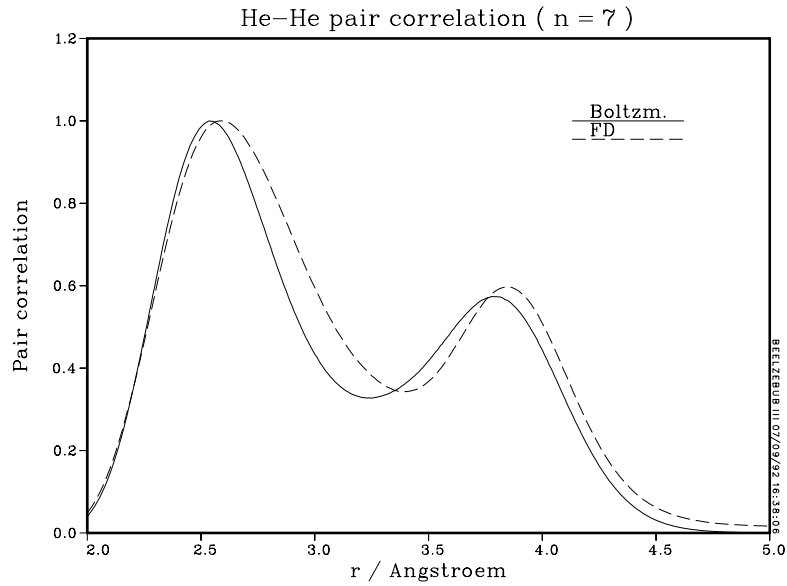


FIG. 6. He-He pair correlation function for $\text{Li}^+ \text{He}_7$.

V. CONCLUSIONS

Albeit the fact that magic numbers are governed through classical potential minima, quantum statistics effects are not negligible. Further studies for $X_M^3\text{He}_N$ clusters including crystal growth, phase transitions etc. may be very interesting. The Path Integral Monte Carlo Method is well suited for the quantum mechanical many body problem. Further development of the method including the quantum mechanical treatment of electrons and nuclei may yield new insight into effects like electron-phonon coupling, etc. in clusters as well as in bulk matter.

REFERENCES

- [1] G.Franke, E.R. Hilf, L. Polley : Z. Phys. **D 9**, 343 (1988)
- [2] M.V. Rama Krishna, K.B. Whaley: Phys. Rev. Lett. **64**, 1126 (1990)
- [3] D.M. Brink, S. Stringari: Z. Phys. **D 15**, 257 (1990)
- [4] V. Staemmler: Z. Phys. **D 16**, 219 (1990)
- [5] G.Franke, J. Schulte : Z. Phys. **D 12**, 65 (1989)
- [6] J. Schulte: Z. Phys. **D 20**, 147 (1991)
- [7] G. Franke, E.R. Hilf, P. Borrmann: *accepted by* J. Chem. Phys. (1991)
- [8] M.V. Rama Krishna, K.B. Whaley: J. Chem. Phys. **93**, 746 (1990)
- [9] S. Nakaichi-Maeda: J.Chem.Phys. **77** (11), 5581 (1982)
- [10] R.P. Feynman, A.R. Hibbs : Quantum Mechanics and Path Integrals New York: McGraw Hill 1965
- [11] U.E. Senff , P.G. Burton: Mol. Phys. **58** (**3**) , 637 (1986)
- [12] M. Takahashi, M. Imada : J. Phys. Soc. Jpn. **53**, 963 (1984)
- [13] M. Takahashi, M. Imada : J. Phys. Soc. Jpn. **53**, 3765 (1984)
- [14] M. Imada : J. Phys. Soc. Jpn. **53**, 2861 (1984)
- [15] J.D. Doll, D.L. Freeman : J. Chem. Phys. **80**, 2239 (1984)
- [16] J.D. Doll, D.L. Freeman : J. Chem. Phys. **80**, 5709 (1984)
- [17] R.D. Coalson, D.L. Freeman, J.D. Doll : J. Chem. Phys. **85**, 4567 (1986)
- [18] A. Giansanti, G. Jacucci: J. Chem. Phys. **89**, 7454 (1988)
- [19] J. Cao, B.J. Berne: J. Chem. Phys. **91**, 6359 (1989)

- [20] K.J. Runge, G.V. Chester: Phys. Rev. **B 38**, 135 (1988)
- [21] M.F. Trotter : Proc. Am. Math. Soc. **10**, 545 (1959)
- [22] N. Metropolis, A. Rosenbluth, M.N. Rosenbluth, A.H. Teller, E. Teller :
J. Chem. Phys. **21**, 1087 (1953)

Kapitel 9

The structure of Small Clusters: Multiple Normal-Modes Modell

The Structure of Small Clusters: Multiple Normal-Modes Model

G. Franke and E. R. Hilf

University of Oldenburg, Physics Dept., P.O.B. 2503, D-W2900 Oldenburg, FRG

P. Borrmann

University of Bremen, Physics Dept., P.O.B. 330440, D-W2800 Bremen, FRG

Abstract

A simple model for the structural fluctuations, isomerizations, and phase transitions of small rare-gas clusters is defined (multi-normal-mode model) which studies the statistical equilibrium of several isomers making use of the normal mode expansion of the free energy. It is evaluated classically and quantum mechanically and its results are compared to those of extensive (path integral) simulation calculations.

I. INTRODUCTION

Small atomic clusters, accessible by experiments give a unique chance to study atomic matter under conditions inaccessible to bulk matter. This field has contributed to the understanding of very different fields such as finite size metal to nonmetal transition, small scale vs. small particle numbers, quantum fluctuations in equilibrium isomerism, thermal equilibrium oscillations,.. [1-6] Triggered by the interesting and unexpected results of mass spectrometry- and other experiments in recent years many theoretical and computer-experimental

investigations of structure and thermal behavior of rare-gas clusters have been carried out. Usually a Lennard-Jones (LJ) potential-model is used to describe the interaction of the atoms the cluster consists of.

The simplest way to gain insight into the questions of structure and stability is the localization of the absolute energy minimum in the N -particle configuration space which will be referred to as BSC (best single cluster). This has been done by numerical methods [3,7] or by the construction of nucleation sequences [4,8]; for smallest clusters – to which we will constrain ourselves in this article – an overview of the results is given in [5].

The BSC model describes the cluster at temperature $T = 0$; for low but finite temperature the cluster should only oscillate locally and harmonically around its BSC configuration. Thus the low temperature behavior can be described by taking into account the normal-mode oscillations [2] of the BSC as has been done for example by [4].

At higher temperature the cluster configuration may leave the vicinity of the BSC and nonlocal rearrangement takes place. Then also other minima of the N -particle potential (isomers) assume statistical importance. In order to investigate this high-temperature behavior, extensive simulations by Molecular Dynamics- and Monte-Carlo-Methods [6,10,12,11,13] have been carried out. The main subject of these works have been the structural transitions the clusters undergo with increasing temperature.

The results show that many different kinds of behavior are possible ranging from isomerizations (the BSC is replaced by another isomer) to more melting-like transitions. As a paradigm for the second kind, the Ar_{13} -cluster has been investigated very intensively; special procedures have been used for the recognition of the involved isomers [12]. For the interpretation of the simulation results Berry et al. [9] proposed a semi-phenomenological model that works with the coexistence of solid and fluid phase in clusters.

In this article we will discuss the behavior of the cluster in a temperature range between these high- and low-temperature regimes: the (thermal) energy is assumed to be larger than the gap between the BSC and higher isomers, but small enough to cause long relaxation times for isomer transformations. In this case the statistical contributions of configurations “between” the isomers are negligible and the configuration space can be considered to be composed of isolated parts in the vicinity of the thermally excited isomers. This conception is supported by experience gained by the observation of the structure fluctuations during simulation calculations. For many cluster sizes MC- as well as in MD-calculations exhibit long phases of only local oscillations interrupted by sudden events of nonlocal rearrangement [12]. The temperature range of this behavior depends on the cluster size and the atomic interaction; in many cases it is larger than the BSC regime. In the second section we define a model which deals with the thermal cluster behavior in this temperature range; in the third section we will compare its results for two examples with those of Monte-Carlo-simulations; in the fourth section two modifications of the model will be discussed.

II. DEFINITION OF THE MODEL

In the multi-normal-modes- (MNM-) model described here we take into account several isomers of a cluster, any of it characterized by its binding energy, permutational degeneracy and normal-mode spectrum. The simplest way to describe the equilibrium of the isomers is to assign an equal amount of entropy (phase-space-volume) to every isomer and to calculate the equilibrium distribution with respect to the energies E_i of the isomers [13]. This method is appropriate to give an idea of which isomers are important, but quantitatively the results on energy and transition temperatures differ from those of simu-

lation calculations. One should expect more precise results from a method that takes the different entropies of the isomers into account using the free energy $F_i = E_i - TS_i$ for the equilibrium distribution. We approximate the entropy by calculating the normal-mode partition function Z_i of every isomer and obtaining the total partition function as the sum of the Z_i .

The correct summation of the contributions of the isomers requires the permutational degeneracy D_i of the isomers taken into account to be known. For example, starting at a triangle there are three ways to construct a quadrangle but only two ways to construct a tetrahedron. By the following argument we obtain the relative degeneracy, that is the ratio $\sigma_i = D_i/D_1$ where D_1 is the degeneracy of the BSC isomer.

Clusters that can be mapped on each other by rotation or particle permutation are considered to be identical; so the “number” of rotations and permutations “cancels out” from the relative degeneracy. But for clusters with rotational symmetry a symmetry rotation maps the cluster on itself exchanging the particles (apart from the rotation axis) and thus is equivalent to a certain permutation. In that case all symmetry rotations have been “canceled out” doubly. To compensate this we have to multiply by their number, i.e. the order of the rotational symmetry-group R_i of the isomer,

$$\sigma_i = \frac{D_i}{D_1} = \frac{R_1}{R_i} . \quad (1)$$

An exact derivation of the above equation was given by Natanson, Amar and Berry [9].

For the statistical equilibrium of isomers, the calculated one-isomer partition functions have to be multiplied by this factor. In order to relate all of them to a common energy (all particles free) also the exponential of the binding energy E_i appears as a relative weight between configurations,

$$Z = \sum_i \sigma_i e^{\beta E_i} Z_i . \quad (2)$$

Let — for a given isomer — x_α^i be the i th spatial component of the position of the particle α with respect to its ideal equilibrium position, $x_\alpha^i = 0$ position. For a pure pair interaction depending only on the distance $r_{\alpha\beta}$ of the particles α and β the second order expansion reads

$$V(\mathbf{x}) = \sum_{\alpha>\beta} v(r_{\alpha\beta}) \approx \frac{1}{2} \sum_{\alpha\beta ij} P_{\alpha\beta}^{ij} x_\alpha^i x_\beta^j \quad (3)$$

with the coefficients

$$P_{\alpha\beta}^{ij} = 2\delta_{\alpha\beta} \sum_{\gamma \neq \alpha} \left[\delta_{ij} v'(\alpha, \gamma) + 2(x_\alpha^i - x_\gamma^i)(x_\beta^j - x_\gamma^j) v''(\alpha, \gamma) \right] \\ - 2(1 - \delta_{\alpha\beta}) \left[\delta_{ij} v'(\alpha, \beta) + 2(x_\alpha^i - x_\beta^i)(x_\alpha^j - x_\beta^j) v''(\alpha, \beta) \right] \quad . \quad (4)$$

v' and v'' being the derivatives of the two-particle potential v with respect to r^2 . The eigenvalues of \mathbf{P}/m are the squares of the normal-mode frequencies ω_k ; due to the six global constants of momentum, and angular momentum six of them are identical to zero. We can now calculate the canonical or micro-canonical, classical or quantum-mechanical partition function of the remaining $3N - 6$ decoupled harmonic oscillators [†].

For the applications of this method discussed below, for v we always used the Lennard-Jones-Potential

$$v(r) = 4\varepsilon \left(\left(\frac{\sigma}{r} \right)^{12} - \left(\frac{\sigma}{r} \right)^6 \right) \quad (5)$$

with parameters appropriate for Argon-Atoms, say $\varepsilon = 10.3\text{meV}$ and $\sigma = 3.405\text{\AA}$, respectively. . The investigated isomers were copied from “snapshots” of MC calculations or constructed “by hand” and relaxed numerically until the internal forces were smaller than $10^{-12}\varepsilon/\sigma$. Then the matrix \mathbf{P} was calculated and diagonalized numerically. The disappearance of the six zero modes has turned out to be a good test of the accuracy of isomer configurations.

III. ISOMERIZATIONS AND MELTING

As the model restricts the motion of the cluster particles to that of a system of independent harmonic oscillators, it enables us to calculate the MNM-partition function for the canonical and microcanonical ensemble. At first we will discuss the case of thermal equilibrium and compare the results with those of corresponding MC calculations [*]. With ω_k^i being the k -th eigenfrequency of the i -th isomer, the MNM-partition function is

$$Z = \sum_i \sigma_i e^{\beta E_i} \prod_{k=1}^{3N-6} \frac{2\pi}{\beta \omega_k^i} . \quad (6)$$

The energy expectation $\langle E \rangle$ and the isomer distribution w_i , i.e. the probability to find the cluster in the configuration of isomer i is

$$\langle E \rangle = \frac{1}{Z} \sum_i Z_i \left(\frac{3N-6}{\beta} - E_i \right) , \quad w_i = \frac{Z_i}{Z} . \quad (7)$$

As a paradigm of a well isolated isomerization we will at first discuss the transition of the Ar_6 -Cluster from its octahedral BSC Structure to an isomer that can be considered to be composed of three tetrahedra (see fig. 1) and thus will be referred to as “tri-tetrahedron”. The binding energies are 12.71ε and 12.30ε , respectively; the rotational symmetry group of the octahedron is of the order $R_{\text{octa}} = 24$, while for the tri-tetrahedron there is only one symmetry rotation of 180° : $R_{\text{tt}} = 2$. The normal-mode spectrum of the tri-tetrahedron (fig. 1) contains rather low frequencies which lead to an increase of entropy and thus favour this isomer at higher temperature. In order to check the reliability of the model, we compare the results to those of Metropolis-MC-calculations carried out with a Fourier-Path-Integral Method suitable for classical as well as for quantum particles. (For details of this method see [13].) The number of used iterations depends on the rate of convergence and ranges from 10^5 to 3×10^6 .

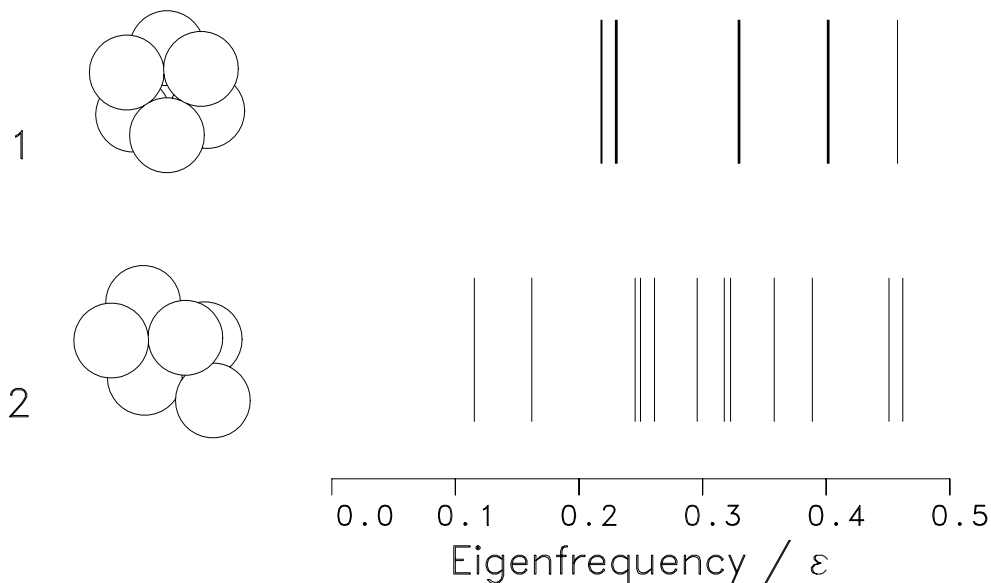


FIG. 1. Most important isomers of Ar_6 : octahedron and tri-tetrahedron and their normal-mode spectra.

While the energy expectations are calculated directly by this method, the isomer distribution is obtained only indirectly from the pair correlation function

$$\Gamma(r) = \left\langle \frac{2}{N(N-1)} \sum_{\alpha < \beta}^N \delta([\mathbf{x}_\alpha - \mathbf{x}_\beta] - r) \right\rangle . \quad (8)$$

It is the probability distribution for finding two arbitrary particles with distance r .

As shown in figure 2, the probability distribution exhibits at low temperatures (besides the nearest-neighbour-peak) only one next-nearest-neighbour peak corresponding to the distance of diagonally opposite corners of the octahedron. The tri-tetrahedron is represented by another second peak which comes up at higher temperature and is clearly distinguishable from the first one. As can be easily checked, both isomers have the same number of next-nearest-neighbour-pairs; thus their statistical weight is directly proportional to the area under the respective peak. Although the choice of the range of each peak is somewhat arbitrary, it has only little influence on the results; we used

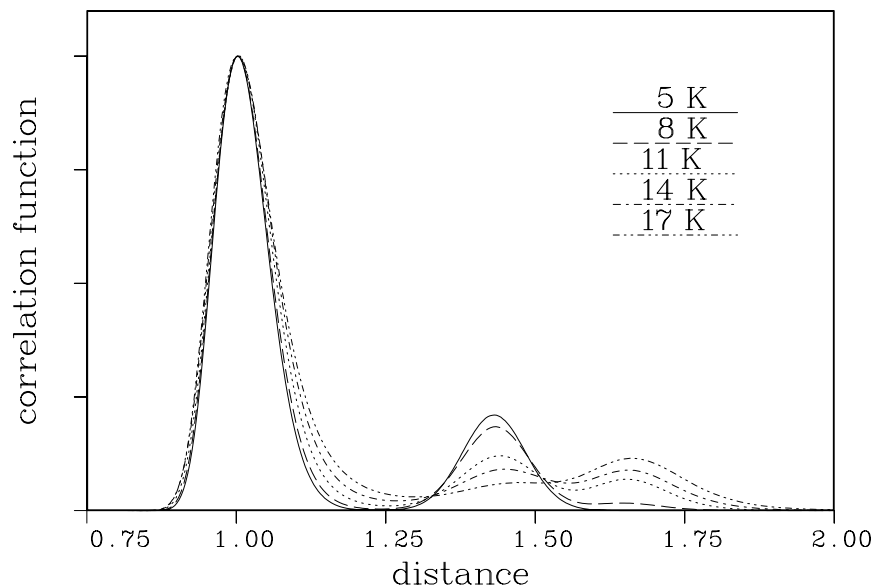


FIG. 2. Pair correlation functions (arb. units) of Ar_6 , distance in units of $r_0 = 2^{1/6}\sigma$.

1.28 r_0 for the beginning of the first peak and 1.59 r_0 for the boundary between the peaks.

The results of the two methods are shown in figures 3 and 4. As expected in the low-temperature region, the energy expectations of the MNM model fit those of the MC-calculations very well. For higher temperature, the MC-values are underestimated as the anharmonic hardcore of the Lennard-Jones potential becomes more important. This turns out to happen in the temperature range where the non-BSC contributions begin to influence the curve. Thus the estimates of the MNM model for the energy expectations seem not to describe the isomerization very well.

On the other hand, the inaccuracy of the energy estimates partially cancels out in the calculation of the isomer distribution. As figure 4 shows, the predictions of the MNM model are in good correspondence with the results of the computer experiments obtained by the procedure described above. In particular the model seems to be able to predict transition temperature and width of the transition range of the isomerization.

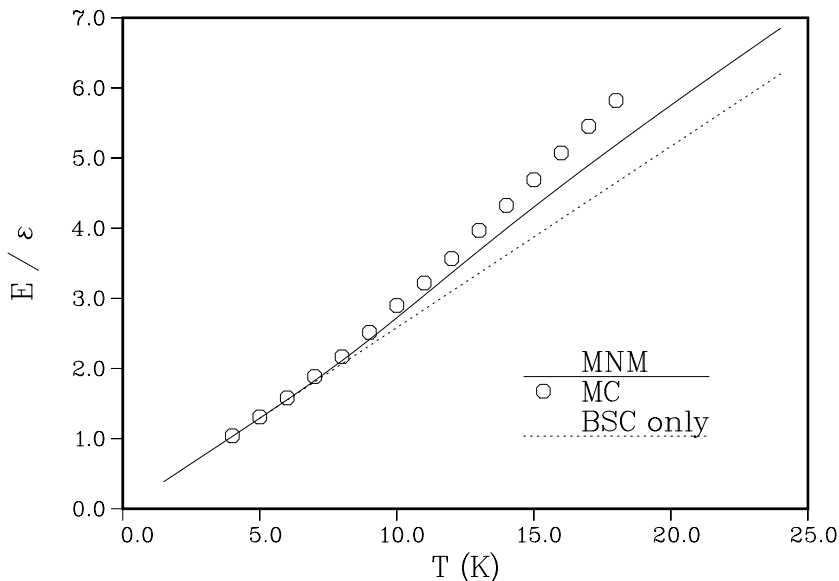


FIG. 3. Energy expectation of Ar_6 from the MNM-model and MC-calculations. The dotted curve represents the BSC-contribution.

As the MC calculations have been carried out without a constraining potential, particles begin to evaporate from the cluster at temperatures above ≈ 20 Kelvin. Thus no simulation data are available for this range and the high-temperature limit of the BSC contribution of $R_{\text{okta}}/R_{\text{tt}} = 1/12$ is not reached. On the other hand, online inspection of the configurations during the MC iterations seem to confirm that no other isomers contribute to the partition function.

As another example of the application of the MNM model but with a more complicated behavior is the transition that Ar_{13} -clusters undergo at a temperature between 30 and 40 Kelvin. In the highly symmetric BSC-configuration of this cluster the first icosahedron shell is closed. This causes a large energy gap between this isomer and the other ones, because the compact shell has to be broken up.

In fact the lowest isomers are singly and doubly decorated icosahedra, i.e. one or two particles are removed from the shell of the pure icosahedron and bound elsewhere on its surface [5]. Although three different singly decorated

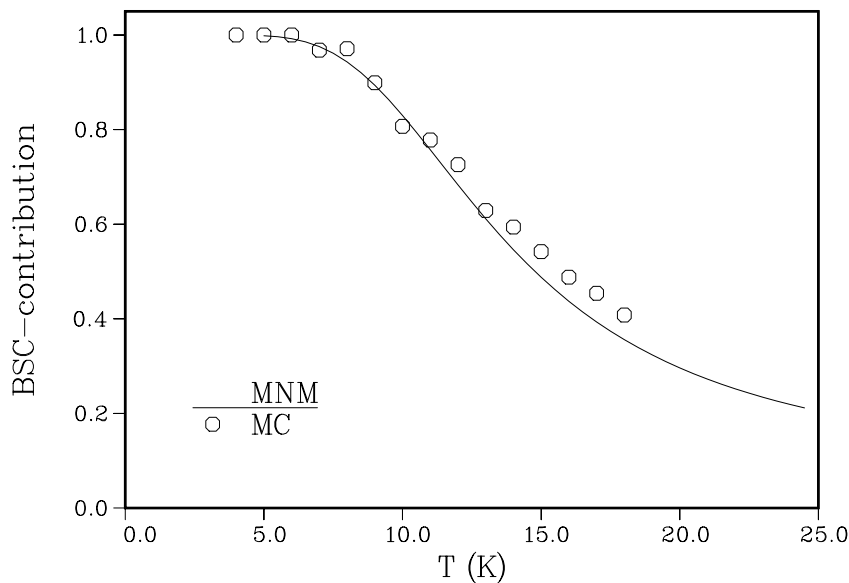


FIG. 4. Isomer-distribution of Ar_6 : relative weight of the BSC-configuration.

isomers exist (distinguished by the distance between decorating particle and “hole”) they can be treated as one, because their binding energies are about equal. The icosahedral symmetry of order 60 is completely broken in all three cases, thus $R_{\text{sdi}} = 180$.

In the case of double decoration one has to distinguish if particles and “holes” are at neighbouring or at distinct positions. An estimation of energy gaps and permutational degeneracy shows that only isomers with neighbouring “holes” are statistically important; the cases of neighbouring and distinct “decorations” have to be treated separately. Table II shows the binding energies and permutational degeneracies times the respective number of isomers of nearly equal energy, and figure 5 the corresponding spectra of eigenfrequencies.

For the higher temperatures where the transition takes place the MNM model again underestimates the thermal energy (figure 6), but the transition temperature – which is indicated by the change of the slope of the curves – seems to agree with the value taken from computer experiments. It is not that

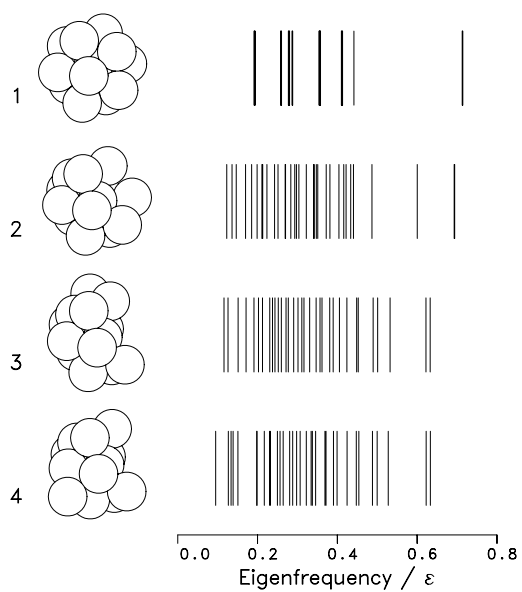


FIG. 5. Most important isomers of Ar_{13} : pure (1), singly decorated (2), and doubly decorated (3,4) icosahedra.

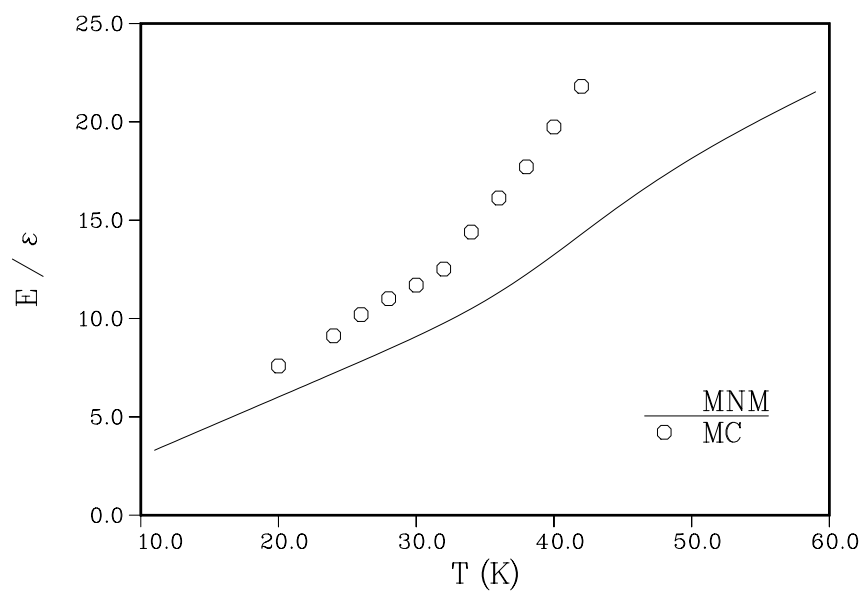


FIG. 6. Energy expectation of Ar_{13} from the MNM model and MC calculations.

Isomer	$E_{\text{bind}}/\varepsilon$	R	κ
pure icosahedron	44.33	1	6.462
singly decorated	41.47	180	6.000
doubly dec., neighb.	40.62	900	5.846
doubly dec., dist.	39.71	4800	5.692

TABLE I. Most important isomers of Ar_{13} with binding energy E_{bind} , permutational degeneracy R , and mean coordination number κ .

easy as in the case of Ar_6 to observe the transition directly in the pair correlation function, because the peaks of this function merge at higher temperature. Only the nearest-neighbour peak is always well distinguished from the other ones. Thus the isomer distribution cannot be calculated directly. However, due to the high compactness of the icosahedral BSC configuration an indirect approach is possible.

As the higher isomers are decorated icosahedra, the decorating atom(s) have less nearest neighbours than the others, i.e. the mean coordination number κ is reduced compared to the icosahedron. If the integral of the correlation function A_{total} is normalized to the total number of particle pairs $N(N-1)/2$, the area under the nearest-neighbour peak A_1 has to be divided by $N/2$ to yield the κ . This will be compared to the prediction of the MNM model:

$$\langle \kappa^{\text{MC}} \rangle = \frac{A_1}{A_{\text{total}}}(N-1) \quad , \quad \langle \kappa^{\text{MNM}} \rangle = \frac{\sum_i \kappa_i Z_i}{\sum_i Z_i} \quad (9)$$

where κ_i is the mean coordination number of the respective isomer (see table II).

The respective results are shown in figure 7. Although the onset of the transition is at the same temperature, the simulation data decrease much more rapidly with increasing temperature. The mean coordination number becomes smaller than the smallest one of the isomers taken into account in the MNM.

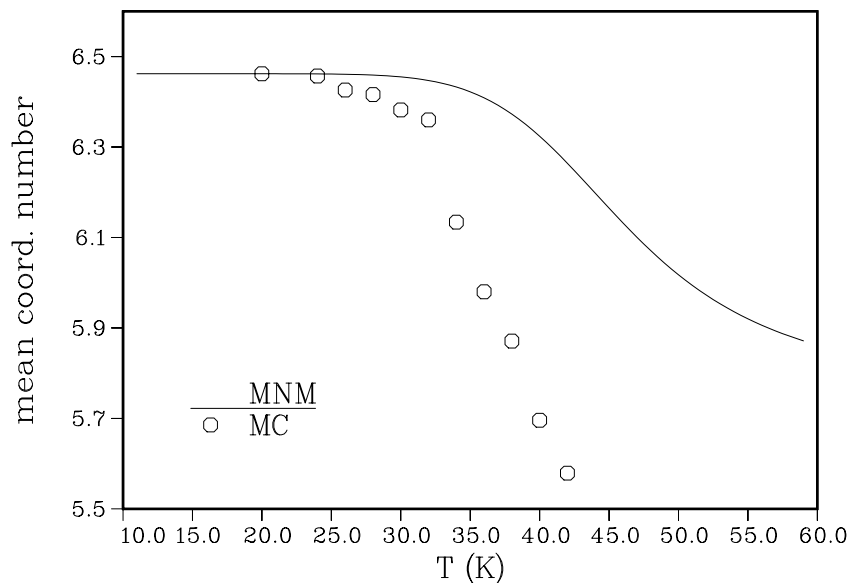


FIG. 7. Mean coordination number of the Ar_{13} -cluster as indicator for the isomer distribution.

Probably this is not due to “forgotten”, isomers because the change of κ is already relatively large for the four isomers considered here (at least three bounds are broken up).

Such a strong effect can only be caused by unstable configurations with one or more particles only bound to one or two atoms of the cluster. The increasing statistical importance of these looser configurations is due to the increasing rate of isomer transformations which leads to a longer time the cluster spends in configurations “between” the isomers. This effect can be understood by two reasons:

- Energy: Because of the high transition temperature the height of the potential barriers between the isomers is small compared to the respective energy gap; so the relaxation times are short just at the onset of the structural transition.
- Entropy: As several isomerizations with high permutational degeneracy and many different realizations of the isomers take place nearly at the

same temperature, a large number of transformation paths through configuration space between the isomers becomes available for the cluster. Thus the phase space volume for configurations besides those of the isomers grows immediately and the increasing entropy leads to a higher statistical weight of these states.

Despite the different nature of the transition of Ar_{13} which is much more melting-like than the isomerization of Ar_6 , the temperature where it takes place seems to be determined by the equilibrium of distinct isomers. The energy- and entropy arguments discussed above – which mark the difference between the two cases – are applicable only above the transition; thus the MNM model gives still good estimates for the onset of the structural transition in both cases.

IV. ALTERNATIVE METHODS OF EVALUATION

As the central idea of the MNM model – local approximation of the most important regions of the energy surface – works on a very basic level, one can make use of it not only in the framework of classical Boltzmann statistics as described above. In this section we will briefly discuss two alternative methods of evaluation of the model: micro-canonical and quantum-mechanical MNM modifications.

Many authors are working with Molecular Dynamics (MD) simulations of cluster dynamics, i.e. in the classical micro-canonical ensemble. One of the most important observables is the average of the kinetic energy $\langle E_{\text{kin}} \rangle$ which is used to calculate an effective Temperature $T = \frac{2\langle E_{\text{kin}} \rangle}{(3N-6)k}$.

In order to interpret the MD results with the help of the MNM model, at first one has to calculate the microcanonical MNM partition function for one isomer from the phase space integral:

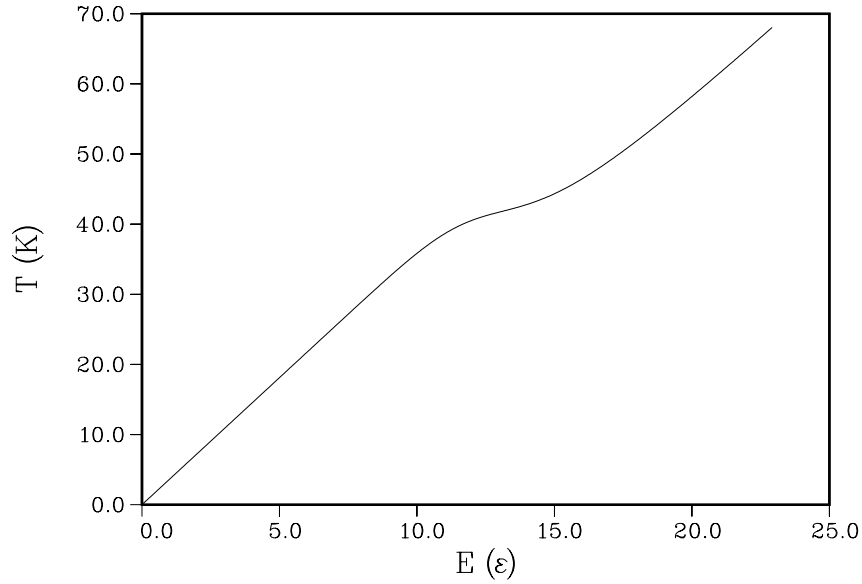


FIG. 8. $T(E)$ curve from the microcanonical MNM model for Ar_{13} .

$$Z_i^\mu(E) = \int (dp dq)^{3N-6} \delta(\varepsilon(q, p) - E) \quad (10)$$

$$= O_{6N-12} \frac{1}{2E} \prod_{k=1}^{3N-6} \frac{2E}{\omega_k^i} \quad (11)$$

where O_n is the surface of the n -dimensional unit sphere. To obtain the MNM partition function, all isomer partition functions have to be related to a common reference energy, and summed up with the relative permutational degeneracies σ_i (eq. 1):

$$Z^\mu(E) = \sum_i \sigma_i Z_i^\mu(E - E_i) \quad (12)$$

The average of the kinetic energy can be obtained by making use of the virial theorem which is true for every isomer: $\langle E_{\text{kin}} \rangle = \frac{1}{2}(E - E_i)$. The total kinetic energy of the cluster is thus

$$\langle E_{\text{kin}} \rangle = \frac{1}{2} \sum_i (E - E_i) \frac{Z_i^\mu}{Z^\mu} \quad (13)$$

As an example the resulting $T(E)$ curve for the case of Ar_{13} is displayed in figure 8. It exhibits the well-known “melting loop” but – as expected – less distinct than the curves obtained from MD data (see for example [11]). Also

transition energy and temperature seem to be in agreement with the data from the corresponding computer experiments.

Although the rare-gas atoms as constituents of Lennard Jones clusters are relatively heavy particles, quantum effects cannot be neglected a priori, because the binding energies are relatively small and zero-point energy as well as energy-level spacing may be in the same order of magnitude. To discuss the importance of quantum effects, the MNM model can be treated as a system of quantum mechanical oscillators.

We use Boltzmann statistics to describe the system, i.e. we consider the atoms as distinguishable particles. Thereby effects which are due to the Pauli principle are neglected. Doing that is justified by recent Path Integral Monte Carlo Calculations of Borrmann and Hilf [16] which show that Pauli Principle effects can be neglected up to the case of the much lighter and weaker bound Neon clusters .

The zero-point energies of the isomers can be calculated directly from the normal-mode spectra. Table III shows them for all isomers discussed above in relation to the total binding energy; the order of magnitude seems to be always about 13% – 15%.

Isomer	$E_{\text{bind}}/\varepsilon$	R	κ
pure icosahedron	44.33	1	6.462
singly decorated	41.47	180	6.000
doubly dec., neighb.	40.62	900	5.846
doubly dec., dist.	39.71	4800	5.692

TABLE II. Most important isomers of Ar_{13} with binding energy E_{bind} , permutational degeneracy R , and mean coordination number κ .

As the energy gaps between the ground states of the isomers are reduced by the zero-point energy, one could expect an influence on isomerizations; they

Particles	Isomer	E_0/ε	E_0/E_{bind}
6	octahedron	1.88	14.8 %
	tri-tetrahedron	1.81	14.7 %
13	pure icosahedron	5.67	12.8 %
	singly decorated	5.43	13.1 %
	doubly dec., neighb.	5.42	13.3 %
	doubly dec., dist.	5.31	13.4 %

TABLE III. Normal-mode zero point energy (E_0) of the isomers discussed above.

should take place at lower temperature than predicted by the classical MNM model. In order to investigate this question we calculate the isomer distribution with the help of the quantum mechanical canonical partition function of the model:

$$Z^{\text{qm}} = \sum_i \sigma_i e^{\beta E_i} \prod_{k=1}^{3N-6} \frac{2}{\sinh(\beta \hbar \omega_k^i / 2)} \quad (14)$$

Figure 9 shows the relative weight of the octahedral BSC configuration Z_1/Z of the Ar_6 cluster in the classical and quantum case. The third curve is calculated classically with the energy gap modified in the sense discussed above and thus demonstrates the isolated effect of the zero-point energy (neglecting the discreteness of states).

It turns out that there is in fact a clear effect due to the zero-point oscillations but it is overcompensated by the discreteness effects. This result is confirmed by quantum-mechanical Monte-Carlo calculations [13]. On the other hand, the reason of this compensation is not clear from the model and the effect may not be generalized to other clusters. (For Ar_{13} no quantum effects occur because of the high transition temperature.)

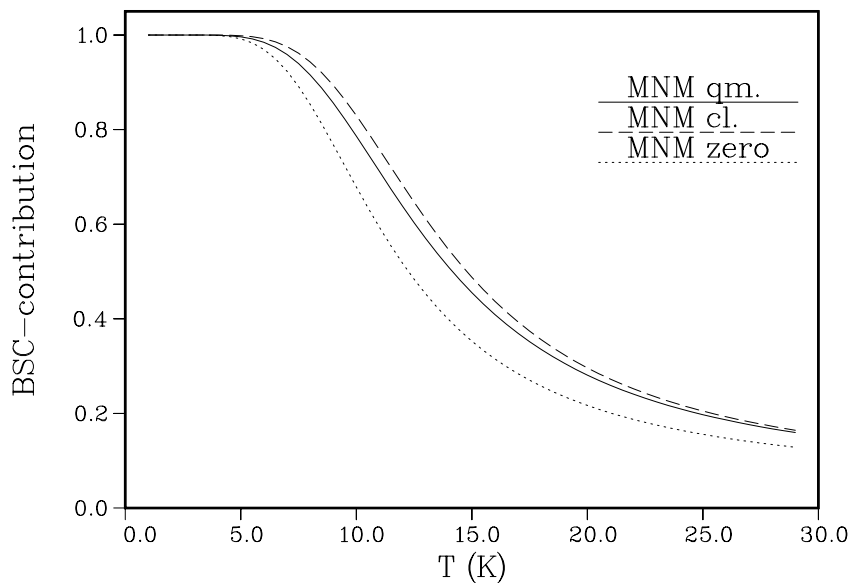


FIG. 9. Relative weight of the BSC-configuration of Ar_6 calculated classically (cl.) and quantum-mechanically (qm.) and the isolated effect of the zero-point energy (zero).

V. CONCLUSIONS

It has been demonstrated that the MNM model gives a realistic picture of the structure of small clusters at moderate temperatures. It can be used as a simple and useful tool for the interpretation of extensive Molecular Dynamics or Monte Carlo simulations. As the temperature/energy estimates for structural transitions of the cluster are approximately correct, one can especially expect to understand these processes. The model provides a criterion (number and degeneracy of important isomers) to predict also, whether the structural transition is isomerization- or melting-like.

The model requires detailed knowledge about the energy surface of the N -particle system. For Lennard-Jones clusters this has been collected in a systematic way, but nevertheless the model is not constrained to this interaction. For example, recent investigations of the Gupta model for transition metal clusters [14] show that also for different potential models the same iso-

mers determine the thermal behavior of the cluster.

An enhanced MNM model may be used to study the importance of quantum statistics for clusters in the future. The problem of evaluating the quantum statistical partition function may be solved by new recursion formulas given by Borrmann and Franke [15], for which the numerical effort to evaluate the partition function only increases approximately with N^2 .

REFERENCES

- ¹ F.F. Abraham: Homogenous Nucleation Theory.
New York, London: Academic Press 1974
- ² M. Weissbluth: Atoms and Molecules.
New York, London: Academic Press 1978
- ³ M.R. Hoare, P. Pal: Adv. Chem. Phys. **20**, 161 (1971)
- ⁴ M.R. Hoare, P. Pal: J. Crystal Growth **17**, 77 (1972)
- ⁵ M.R. Hoare, Adv. Chem. Phys. **40**, 49 (1979)
- ⁶ C.L. Briant, J.J. Burton: J. Chem. Phys. **63**, 2045 (1975)
- ⁷ J. Farges, M.F. de Feraudy, B. Raoult, G. Torchet:
J. Chem. Phys. **78**, 5067 (1983)
- ⁸ J. Farges, M.F. de Feraudy, B. Raoult, G. Torchet:
Surf. Sci. **156**, 370 (1985)
- ⁹ G. Natanson, F. Amar, R.S. Berry: J. Chem. Phys. **78**, 399 (1983)
R.S. Berry, J. Jellinek, G. Natanson: Chem. Phys. Lett **107**, 227 (1984)
- ¹⁰ F.G. Amar, R.S. Berry: J. Chem. Phys. **85**, 5943 (1986)
J. Jellinek, T.L. Beck, S. Berry: J. Chem. Phys. **84**, 2783 (1986)
T.L. Beck, J. Jellinek, S. Berry: J. Chem. Phys. **87**, 545 (1987)
T.L. Beck, S. Berry: J. Chem. Phys. **88**, 3910 (1988)
R.S. Berry: Z. Phys. D **12**, 161 (1989)
- ¹¹ H.L. Davis, J. Jellinek, S. Berry: J. Chem. Phys. **86**, 6456 (1987)
- ¹² E. Blaisten-Barojas, E. Garzon, I.L. Avalos-Borja:
Phys. Rev. B **36**, 8447 (1987)

- E. Garzon, I.L. Avalos-Borja, E. Blaisten-Barojas: *Z. Phys. D* **12**, 181 (1989)
- ¹³ G. Franke, E. R. Hilf, L. Polley: *Z. Phys. D* **9**, 343 (1988)
G. Franke, J. Schulte: *Z. Phys. D* **12**, 65 (1989)
- ¹⁴ S. Sawada, S. Sugano: *Z. Phys. D* **14**, 247 (1989)
- ¹⁵ P. Borrmann, G. Franke: preprint, Universität Oldenburg, 1992
P. Borrmann, G. Franke, private communication
- ¹⁶ P. Borrmann, E.R. Hilf: Thermal properties of Ne clusters at low temperatures, in preparation;
J. Curdes, P. Borrmann, E.R. Hilf, W. Tuszynski: Computer Analysis Tools for PDMS spectra; ASMS (Symp. Am. Soc. Mass Spectrometry; Washington D.C. (1992));
- * Strictly speaking, isolated clusters (no external pressure) are thermally unstable, thus the term “thermal equilibrium” can only be applied to clusters with internal relaxation times much smaller than their mean lifetime. The thermal picture describes the behavior in time scales which are small compared to lifetime.
- † In the special case of a linear equilibrium configuration there are only five zero eigenvalues of \mathbf{P} .

Danksagung

Ich danke Herrn Prof.Dr.Dr. E.R. Hilf für die Betreuung dieser Arbeit, viele wertvolle Anregungen, kritische Diskussionen und persönliche Anregungen. Mein Dank gilt auch den Mitgliedern der Arbeitsgruppe Theorie III des Fachbereichs Physik der Carl von Ossietzky Universität Oldenburg und des Institutes für Theoretische Physik der Universität Bremen für viele anregende Diskussionen und stetiges Interesse an dieser Arbeit.

Die teilweise sehr umfangreichen Rechnungen wurden auf IBM RISC Workstations der Fachbereiche für Physik der Universitäten Bremen und Oldenburg sowie auf dem Siemens/Fujitsu S400 Höchstleistungsrechner des *Regionalen Rechenzentrums für Niedersachsen* (**RRZN**) in Hannover durchgeführt.

Curriculum vitae

Name: Peter Borrmann
Geburtsdatum: 5.Mai.1965
Geburtsort: Gelsenkirchen
Staatsangehörigkeit: deutsch

Schule

1971-1972	Grundschule an der Georgstraße in Gelsenkirchen
1972-1974	Volkschule Bengersiel
1974-1975	Grundschule Esens
1974-1976	Orientierungsstufe Esens
1976-1984	Niedersächsisches Internatsgymnasium in Esens Abschluß mit Abitur (Note: 1.6)
1984 -1985	Zivildienst beim Rettungsdienst Friesland in Jever

Studium

1985-1988	Grundstudium der Physik und Mathematik, Universität Oldenburg Erwerb des Vordiploms in Physik (Note : sehr gut)
1988-1990	Hauptstudium der Physik, Universität Oldenburg
5/90-12/90	Diplomarbeit bei Prof.Dr.Dr.Hilf, Universität Oldenburg
2/91	Abschluss mit Physik-Diplom (Note: sehr gut)

Berufstätigkeit

5/91-6/91	Wissenschaftlicher Mitarbeiter, Universität Oldenburg (Präsidentenfonds)
seit 3/91	Doktorat bei Prof.Dr.Dr. Hilf, Universität Oldenburg zum Thema: "Pathintegral methods and applications to cluster physics" (Arbeitstitel)
7/91-9/93	Wissenschaftlicher Mitarbeiter (Projekt: Fachinformation in der Physik), Universität Bremen
seit 10/93	Wissenschaftlicher Mitarbeiter , Universität Oldenburg

Erklärung nach §8(2) der Promotionsordnung:

Teil 1 dieser Arbeit wurde von mir selbständig verfaßt.
Die in den Kapitel 2-8 enthaltenen Arbeiten wurden im wesentlichen von mir erarbeitet und verfaßt.
Zu der in Kapitel 6 aufgenommenen Arbeit hat der Student Dorian Gloski Teilrechnungen im Rahmen einer Studienarbeit beigetragen.
Zu Kapitel 7 hat Herr Bernd Diekmann insbesondere sein Wissen zu Hartree-Fock Rechnungen und deren Sensibilität bei der Anwendung auf Übergangsmetallcluster in Diskussionen eingebracht und vermittelt.
Die Arbeiten an dem in Kapitel 9 abgedruckten Artikel wurden unter Federführung von Gert Franke begonnen und von mir beendet.
Die Beiträge der von mir als Gutachter vorgeschlagenen E.R. Hilf und D. Tomanek zu den Kapiteln 4,5,7,8,9 bzw. 7, bitte ich von diesen selbst bewerten zu lassen.

Es wurden keine anderen als die in der Arbeit angegebenen Hilfsmittel verwendet.